

**“PREDICTIVE ANALYTICS BASED MICRO-NANO
BUBBLE (MNB) GENERATION FOR EFFECTIVE WATER
TREATMENT”**

**A thesis submitted to the
*University of Petroleum & Energy Studies***

**For the award of
DOCTOR OF PHILOSOPHY
in
*Electrical and Electronics Engineering***

BY

Piniseti Swami Sairam

July 2020

SUPERVISOR (S)

Dr. Jitendra K Pandey

Dr. Ravi Gunupuru



**Department of Electrical and Electronics Engineering
School of Engineering
University of Petroleum and Energy Studies
DEHRADUN-248007: Uttarakhand**

**“PREDICTIVE ANALYTICS BASED MICRO-NANO
BUBBLE (MNB) GENERATION FOR EFFECTIVE WATER
TREATMENT”**

**A thesis submitted to the
*University of Petroleum & Energy Studies***

**For the award of
DOCTOR OF PHILOSOPHY
in
*Electrical and Electronics Engineering***

BY

**Piniseti Swami Sairam
(SAP ID- 500056856)**

July 2020

Supervisor

Dr. Jitendra K Pandey
Professor and Associate Dean
Research & Development
University of Petroleum and Energy Studies

Co-Supervisor

Dr. Ravi Gunupuru
Assistant Professor (SS)
Department of Applied Sciences
University of Petroleum and Energy Studies



UNIVERSITY WITH A PURPOSE

**Department of Electrical and Electronics Engineering
School of Engineering
University of Petroleum and Energy Studies
DEHRADUN-248007: Uttarakhand**

Sep 2020

DECLARATION

I declare that the thesis entitled “**Predictive Analytics Based Micro-Nano Bubble (MNB) Generation For Effective Water Treatment**” has been prepared by me under the guidance of **Dr. Jitendra K Pandey**, Associate Dean, Research & Development, University of Petroleum & Energy Studies and **Dr. Ravi Gunupuru**, Assistant Professor of Department of Applied Sciences, University of Petroleum & Energy Studies. No part of this thesis has formed the basis for the award of any degree or fellowship previously.



Piniseti Swami Sairam

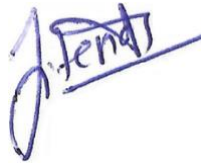
School of Engineering
University of Petroleum & Energy Studies
Dehradun-248007: Uttarakhand

DATE: 14 Sep 2020

CERTIFICATE

We certify that **Piniseti Swami Sairam** has prepared his thesis entitled “**Predictive Analytics Based Micro-Nano Bubble (MNB) Generation For Effective Water Treatment**”, for the award of PhD degree of the University of Petroleum & Energy Studies, under our guidance. He has carried out the work at the Department of Electrical and Electronics Engineering, University of Petroleum & Energy Studies.

Supervisor



Dr. Jitendra K Pandey

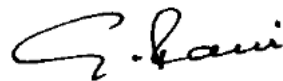
Professor & Associate Dean

Research & Development

University of Petroleum and Energy Studies

Date: 14 Sep 2020

Co-Supervisor



Dr. Ravi Gunupuru

Assitant Professor (SS)

Department of Applied Sciences

University of Petroleum and Energy Studies

Date: 14 Sep 2020

ABSTRACT

With the growing demand of clean drinking water, researchers have long been trying to develop green and sustainable water treatment technologies, which are easily transferrable to the society. Micro-Nano Bubble (MNB) have shown great potential in water treatment and other aligned areas because of their immense oxidation properties. The use of O₃ MNB are considered to be eco-friendly given to its nature to convert back into oxygen after a particular duration. Recently researchers have reported the use of O₃ MNBs for water treatment for removal of contaminations like arsenic and coliform. However, generation and stability of MNBs have posed a serious concern on the real time treatment applications.

Stability of MNBs generated using pressurised decompression method depends majorly on factors such as temperature, gas type, system operating pressure and gas flow rate etc, that may increase the unpredictability and reproducibility of results for effective water treatment.

In the present study, the system was developed to produce MNBs with minimum sensory interventions to determine the size of MNB generated. This was achieved with help of machine learning model approach. A set of experimentations were performed to identify the operations parameters and understand the properties of MNBs and the observations were stored in the form of dataset for developing machine learning models. Further to test the efficiencies of MNB in oxidation process, removal of arsenic and coliform bacteria from water was studied using O₃ MNBs.

The results illustrated the potential of smaller bubbles over larger towards effective oxidation process. It was observed that MNBs generated using Compressed air, oxygen and ozone resulted in 3000-5000nm, 1500-3000nm and 300-1500nm respectively under different operating conditions. In the experimental studies conducted for a duration of 30 mins, O₃ MNBs smaller than 500nm showed better oxidation capability in the case of As. In case of

coliform disinfection, a similar oxidation trend was observed for 700nm O₃ MNBs.

To further explore the possibility of generating a particular MNB without any dependencies on size detecting sensors, machine learning approaches such as decision tree and multi linear regression models were chosen based on the relationships of the parameters. These models showed a possibility of using machine learning based bubble size estimation where it was observed that multi linear regression model showed a prediction error of 5-15 % while decision tree resulted in 20-30% of prediction error.

ACKNOWLEDGMENT

I would like to express my heartfelt gratitude to my supervisors Dr. Jitendra K Pandey and Dr. Ravi Gunupuru, for their continuous encouragement and motivation throughout my research work. I am very thankful to them for introducing me to this promising area of research and for the guidance, which I have been getting all these years of my research.

I would like to show gratitude to Dr. S. J. Chopra (Chancellor), Dr. Sunil Rai (Vice-Chancellor) and Dr. Kamal Bansal (Dean) at the University of Petroleum & Energy Studies for their cherished support for my research work.

Many thanks go to Dr. Kiran Kumar Ravulakollu ,Assistant Dean SoC-R&D, for his constant support throughout my research. I would like to thank the Research Committee members of the School, for their constant and timely inputs. I would like to extend my special thanks to Mr. Amritansh Mehrotra and Mr. Samarth who stood with me at different phases of my work. Special thanks to Dr. S R V S Prasanna, Mr. Caneon Kurien, Mr. Debajyoti Bose and Ms. Aslesha Bodavula for all the discussions and inputs provided. I also thank all my fellow colleagues of R&D department Dr. Surajit Mondal, Mr. Ravi Patel and Mr. Anurag Barmola for their support.

I would like to acknowledge in-house Central Instrumentation Centre (CIC) and Composite Lab facility; where I have carried out my research work. I also thank lab technicians Dr. Devendra Rawat and Mr. Charu Chandra mPant. I would like to express my gratitude to SRE Department and Ms. Rakhi Ruhall for the support extended.

Words cannot express how grateful I am to my parents P. Satyanarayana and P. Lalitha, for showing faith in me and giving me liberty to choose what I desired. I salute you all for the selfless love, care, pain and sacrifice you did to shape my life. My in laws Sunil S and Chitra Sreedhar S, my grandparents S S

P R S Rao and S S P Devi and my relatives for their constant support, love and encouragement and all of the sacrifices that you've made on my behalf. Your prayer for me was what sustained me thus far.

I also take this opportunity to thank my loving wife Meera C S without whom this couldn't been done. You were always around at times I thought that it is impossible to continue, you helped me to keep things in perspective. I greatly value her contribution and deeply appreciate her belief in me. She gave me support and help, discussed ideas and prevented several wrong turns. Thank you for the constant efforts and motivation to keep me focused on my work and inspiration throughout my journey.

To my family

TABLE OF CONTENTS

DECLARATION.....	i
CERTIFICATE.....	ii
ABSTRACT.....	iii
ACKNOWLEDGMENT	v
LIST OF FIGURES	xi
LIST OF TABLES	xiv
ABBREVIATION.....	xv
CHAPTER 1 INTRODUCTION.....	1
1.1 OVERVIEW	1
1.2 SCOPE OF STUDY.....	5
1.3 PRINCIPLE CONTRIBUTIONS	6
1.4 RESEARCH OBJECTIVES	6
1.5 THESIS OVERVIEW.....	6
CHAPTER 2 LITERATURE REVIEW.....	8
2.1 ARSENIC CONTAMINATION	8
2.1.1 ARSENIC REMOVAL METHODOLOGIES	9
2.2 COLIFORM CONTAMINATION.....	13
2.2.1 COLIFORM REMOVAL METHODOLOGIES	15
2.3 MICRO-NANO BUBBLE (MNB) IN WATER TREATMENT	17
2.3.1 PROPERTIES OF MICRO-NANO BUBBLE (MNB)	19
2.3.1.1 SIZE AND SHAPE.....	19
2.3.1.2 RESIDENCE TIME.....	20
2.3.1.3 SELF-PRESSURIZING EFFECT AND RISE TIME	21
2.3.2 GENERATION OF MNB.....	21

2.3.2.1 ROTARY LIQUID FLOW TYPE.....	21
2.3.2.2 VENTURI TYPE.....	22
2.3.2.3 PRESSURIZED DISSOLUTION TYPE.....	23
2.3.2.4 EJECTOR TYPE	23
2.3.2 MICRO-NANO BUBBLE SIZE DETERMINATION	24
2.3.3 APPLICATIONS OF MICRO-NANO BUBBLE	25
CHAPTER 3 MICRO-NANO BUBBLE (MNB) GENERATION	30
3.1 EXPERIMENTAL SETUP.....	30
3.2 MEASUREMENT OF MNB SIZE	31
3.3 EXPERIMENTAL PROCEDURE GENERATION	32
3.3.1 MNB GENERATION.....	32
3.3.2 EXPERIMENTAL CONDITIONS	33
3.3.3 EXPERIMENTAL RESULTS.....	36
3.4 SUMMARY	41
CHAPTER 4 REMOVAL OF ARSENIC AND COLIFORM	42
4.1 REMOVAL OF ARSENIC USING O ₃ MICRO-NANO BUBBLE	42
4.1.1 INTRODUCTION	42
4.1.2 MATERIAL AND METHODS	44
4.1.3 SYNTHESIS OF ADSORBENT.....	44
4.1.4 MEASUREMENT OF AS USING ICP-OES.....	46
4.1.5 RESULTS AND DISCUSSIONS.....	47
4.2 REMOVAL OF COLIFORM USING O ₃ MICRO-NANO BUBBLE..	51
4.2.1 INTRODUCTION	51
4.2.2 MATERIAL AND METHODS.....	52
4.2.3 MEASUREMENT OF COLIFORMS	53
4.2.4 RESULTS AND DISCUSSION.....	53
4.3 SUMMARY	55
CHAPTER 5 MICRO-NANO BUBBLE SIZE PREDICTION.....	56

5.1 OVERVIEW	56
5.2 MACHINE LEARNING APPROACH	57
5.2 COMPUTATION OF MNB	58
5.2.1 RELATIONSHIP BETWEEN THE PARAMETERS.....	60
5.3 LEARNING BASED ESTIMATION.....	61
5.4 ALGORITHM.....	61
5.5 REGRESSION MODELS	62
A. DECISION TREE	62
B. MULTI LINEAR REGRESSION MODEL.....	66
5.5. EVALUATION.....	67
5.6 SUMMARY	74
CHAPTER 6 CONCLUSION AND FUTURE WORK.....	75
6.1 CONCLUSION.....	75
6.2 REMOVAL OF ARSENIC AND COLIFORM FROM WATER.....	76
6.3 MNB SIZE PREDICTION	76
6.4 SCOPE OF FUTURE WORK	76
REFERENCES.....	77

LIST OF FIGURES

Figure 1.1 Sources of Arsenic Contamination into Water [18]	3
Figure 1.2 Sources of Coliform Bacteria Contamination into Water	4
Figure 2.1 Arsenic Intake Medium by Humans [41]	9
Figure 2.2 Classification of Coliform Bacteria.....	13
Figure 2.3 Process of Coliform Bacteria Intake by Humans	15
Figure 2.4 Scanning Electron Microscopy (SEM) images of E.coli; (a) Controlled E.coli; (b) Treated E.coli [84]	16
Figure 2.5 Structure of a Micro-Nano Bubble (MNB)	18
Figure 2.6 Diagram showing macro, micro and nanobubbles[96].....	20
Figure 2.7 Young laplace law [99]	21
Figure 2.8 Rotary liquid flow type MNB generator	22
Figure 2.9 A venturi type MNB generator	22
Figure 2.10 MNB generation through pressurized dissolution method	23
Figure 2.11 Ejector type MNB generator	24
Figure 3.1 Schematic diagram of experimental setup.....	30
Figure 3.2 Experimental setup; (a) Micro-nano bubble generator; (b) Water tank; (c) Rotameter	33
Figure 3.3 MNB generation; (a) immediately after starting the system; (b) after 5 mins of MNB generation	34
Figure 3.4 Structure of MNB; (a) in absence of surfactant; (b) in presence of surfactant.....	35
Figure 3.5 MNBs at 60 PSI.....	36
Figure 3.6 MNBs at 80 PSI.....	37
Figure 3.7 Compressed air MNBs in presence of surfactants.....	38
Figure 3.8 Stability of MNB in presence of surfactants; (a) Oxygen MNB; (b) Ozone MNB	39
Figure 3.9 Observation of lifetime of MNBs in a 5ml cuvette; (a) at time t= 15min; (b) t= 30min; (c) t= 45min; (d) t= 60 min	40

Figure 4.1 Role of bubble size in oxidation rate (a) larger bubble size tend to rise to the surface; (b) smaller bubbles remains in water for longer duration	43
Figure 4.2 Methodology to treat arsenic	43
Figure 4.3 Scanning Electron Microscopy (SEM) analysis of ZrAC adsorbents containing (a) 5.9% zirconyl nitrate solution and (b) 10 % zirconyl nitrate solution	45
Figure 4.4 Experimental setup of adsorbent in a glass column	46
Figure 4.5 ICP-OES instrument calibration graph using As (V) standard at 11 point concentrations	47
Figure 4.6 Oxidation of As(III) to As(V) using different O ₃ MNBs	48
Figure 4.7 O ₃ MNBs performance when As contaminated water is treated and passed through the adsorbent	49
Figure 4.8 SEM-EDX analysis of adsorbent; (a) before adsorption of As(V); (b) after adsorption of As(V); (c) EDX of adsorbent showing presence of As	50
Figure 4.9 XRD analysis of adsorbent before and after adsorption.....	51
Figure 4.10 Methodology to treat coliform bacteria	51
Figure 4.11 Preparation method of nutrient agar media	52
Figure 4.12 Serial dilution procedure of the sample.....	52
Figure 4.13 Culture of E.coli in nutrient agar media; (a) before treatment with O ₃ MNB; (b) after treatment with O ₃ MNB.....	54
Figure 4.14 Removal efficiency of coliform bacteria using O ₃ MNBs	54
Figure 5.1 Methodology of machine learning models	57
Figure 5.2 MNB dataset; (a) data entry form; (b) sample dataset	59
Figure 5.3 Decision tree model to predict MNB size	64
Figure 5.4 Prediction models evaluation for compressed air MNBs of (a) 1500nm; (b) 2000nm; (c) 2500nm; (d)3000nm.....	69
Figure 5.5 Prediction models evaluation for O ₂ MNBs of (a) 1000nm; (b)1500nm; (c)2000nm; (d) 2500nm	71

Figure 5.6 Prediction model evaluation for O₃ MNBs of (a) 300nm; (b) 500nm;
(c) 1000nm; (d) 1500nm73

LIST OF TABLES

Table 2.1 Arsenic Removal Methodologies from Water	11
Table 2.2 Applications of MNB.....	27
Table 3.1 Experimental Parameters	33
Table 3.2 Composition of different surfactants used	35
Table 3.3 Rate of change in MNB size after generation.....	40
Table 5.1 Standard deviation (SD) of attributes	65
Table 5.2 SD reduction of the attributes	66
Table 5.3 Minimum and maximum prediction ranges of MNB ML models...	67

ABBREVIATION

BOD	Biochemical Oxygen Demand
COD	Chemical Oxygen Demand
TSS	Total Suspended Solids
MNB	Micro-Nano Bubble
CTAB	Cetyl Trimethyl Ammonium Bromide
SDS	Sodium dodecyl Sulfate
SEM	Scanning Electron Microscopy
XRD	X-Ray Diffraction
ORP	Oxidation Reduction Potential
CFU	Colony Forming Units
ML	Machine Learning
CART	Classification and Regression Tress
DT	Decision Tree
MLR	Multi Linear Regression
SD	Standard Deviation

CHAPTER 1

INTRODUCTION

1.1 OVERVIEW

Ground and surface water are the two major sources of drinking water supply worldwide. Groundwater is a common source for single homes and small towns, while rivers and lakes are the usual sources for large cities. Although approximately 98 percent of liquid fresh water exists as groundwater. The volume of water available for municipal supply depends mostly on the amount of rainfall and also on the size of the watershed, the slope of the ground, the type of soil and vegetation, and the type of land use. The rapid growth in population has resulted in the scarcity of drinking water, leading to catastrophic water shortage in several areas of the world. Over two billion people still live in countries experiencing high water stress, while four billion people experience severe water scarcity for at least one month a year [1].

Poor water quality exacerbates the issue, with 80% of wastewater globally being returned to the environment untreated. With the world's population set to increase to over ten billion by 2050 from around seven billion today, water demand can potentially increase by more than 70% driven by urbanization and changing consumption patterns in the emerging world [2]. Since only around 0.8% of the total earth's water is fresh water, groundwater resources are being exploited to meet the present demands [3]. It is projected that by year 2030, the global needs of water would increase to 6,900 billion m³ from the current 4,500 billion m³. Thus, about 53% increase in the amount of drinking water is needed by year 2030[4].

In India, the per capita availability of water is estimated to decline further to 1,465 cubic meter by 2025 and 1,235 cubic meter by 2050[5]. Consequently, the present surface water resources will no longer be sufficient to meet the future needs of mankind, while groundwaters were mostly polluted

due to natural phenomena and anthropogenic activities of human. About 85% of rural population in India is solely depended on groundwater, which is depleting at a fast rate. The contamination of groundwater with metals is primarily attributed to anthropogenic activities and requires risk assessment to characterize the magnitude of the threats to humans and ecological receptors[6]. In addition, the natural weathering of soils and rocks also introduce traces of elements into the groundwater.

Water quality monitoring studies carried out by various national and international agencies often report that the freshwater bodies in India contain high levels of organic and microbial pollutants. Though only a few of the chemicals that can occur in drinking water have immediate health effects to humans, priority must be given for monitoring and remedial actions towards chemical contaminants in drinking water in order to ensure its efficient management and avoid adverse health effects associated to prolonged period of exposure [7]–[15].

To date, arsenic in groundwater has been identified in 105 countries, with an estimate of the exposed population of >200 million worldwide at concentrations greater than the World Health Organization (WHO) guideline value for arsenic of 10 µg/L [16]. The major route for arsenic exposure to humans is through drinking water where it is typically present in inorganic forms of either arsenite [As (III)] or arsenate [As (V)] while another significant pathway of arsenic contamination is through the food chain. When contaminated water is used for crop irrigation, it enters the food chain thus, when the crops are being consumed, the people are exposed to arsenic.

India covers 79% of the Ganga River Basin (GRB), is spread across states such as Uttarakhand, Uttar Pradesh, National Capital Territory (NCT) of Delhi, Madhya Pradesh, Bihar, Jharkhand, Rajasthan, Chhattisgarh, Punjab, Haryana, and West Bengal. The GRB is a part of the Ganga-Brahmaputra-Meghna (GBM) river basin, draining 1.08 million km² in Tibet, Nepal, India, and Bangladesh; it covers nearly 26% of India's land mass and is home to a population of over 500 million[17]. Groundwater arsenic contamination in these

areas was first reported in 1976 in Chandigarh and in different villages of the Punjab and Haryana states [17].

Different sources for Arsenic contamination in water is given in fig.1.1.

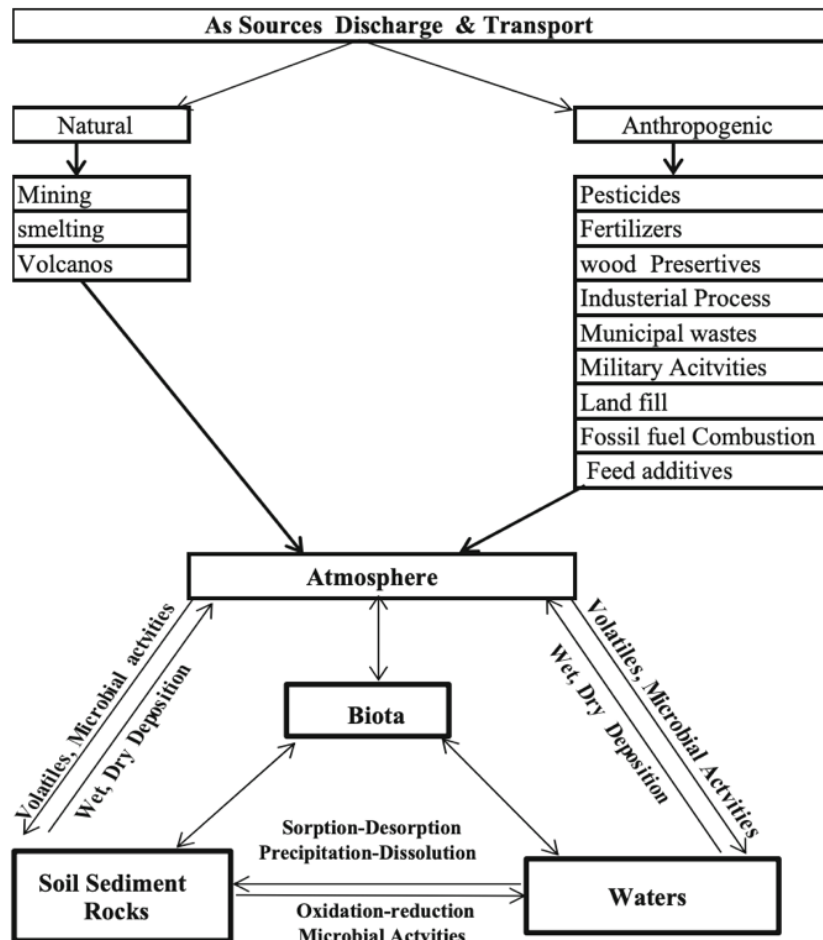


Figure 1.1 Sources of Arsenic Contamination into Water [18]

However, currently available scientific literature reveals that the Ganga is considered to be one of the world's most polluted rivers, containing a number of toxins including arsenic, cadmium, chromium, copper, lead, and mercury, as well as pesticides and pathogenic microbes nearly 3000 times greater than the safe limit prescribed by the World Health Organization (WHO) i.e., 0 CFU for coliform bacteria [17], [19].

Arsenic-related major health hazards through chronic exposure of contaminated groundwater for drinking and cooking have been registered in

several countries and the Asian countries are found to be the most affected [20]. Significantly, microbial contaminants such as coliforms, E.coli, Cryptosporidium parvum, and Giardia lamblia compromise the safety of the water. The prevalence of water-borne diseases including diarrhea, cholera, typhoid fever, and dysentery, has been mainly attributed to unsafe water and unhygienic practices[21], [22].

Waste generated from their activities and runoff from agricultural fields rich in fertilizers, pesticides, insecticides, herbicides, etc. made traditional sources of drinking water unfit for consumption including the holy Ganga water. Presence of Escherichia coli, Klebsiella, and Enterobacter species in water is a likely indicator of the presence of pathogenic organisms such as Clostridium pafringens, Salmonella, and Protozoa. These pathogens are usually found in human and animal feces and could possibly reach the sources of community water supply through leaching or other means such as improperly treated sewage[23]. Different sources of coliform bacteria contamination is illustrated in fig. 1.2.

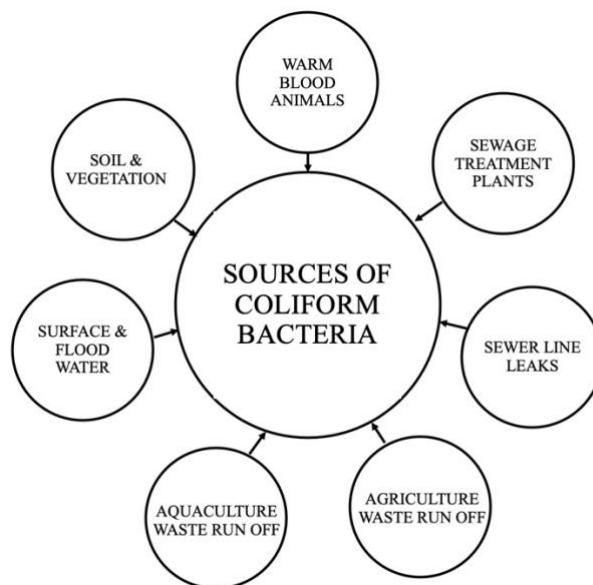


Figure 1.2 Sources of Coliform Bacteria Contamination into Water

Any potable water may be contaminated microbiologically due to insufficient sanitation and unhygienic practices. In order to estimate the number of microbes present and to find out microbial types, different microbiological water analysis methods are used in different labs. It is a very expensive and strenuous procedure to examine all the possible microbial pathogens in water, and therefore, a specific group of microorganisms that come from the same source as human pathogens is used to indicate the presence of pathogens. In order to indicate the presence of faecal contamination in water, indicator microorganisms were approved for the studies of coliform bacteria in the U.S. Public Health Service in 1914[24]. If indicator microorganisms are observed in a substance, it designates the presence of faecal contamination and therefore, pathogenic microorganisms might be present in that water.

1.2 SCOPE OF STUDY

The proposed study will combine micro-nano bubbles and machine learning approach as an integrated treatment process. The research objective of implementing machine learning approach and using MNBs for the effective removal of arsenic and coliform bacteria from water can be divided into three parts; design of MNB generation system, finding the optimal conditions for effective oxidation and ozonation for arsenic and coliform, system learning approach towards automated bubble generation of different sizes.

Studies on MNB have shown its potential and have been effectively used for various applications. Based on the literature, where MNBs were tested for their efficiency, it was observed that determination of the size being generated during operation was a hefty task and required high instrumentation. Although, these studies were carried out in spiked water made with distilled water or millipore water where the presence of external particles are very limited, this limits the study for further upscaling of the system towards water treatment industries for efficient aeration, dissolved air floatation, oil and water separation process, etc., in real time scenarios. Since the technology is implemented mostly

in a recirculation mode; where the water for treatment is itself used as an input source to produce bubble, it becomes a challenging environment for the sensors determining MNB size to differentiate between a waste and a bubble.

Therefore, implementation of learning and prediction methodology can be of potential as the system can be advanced by imparting the difference of a bubble and a waste particle. For an efficient implementation of learning and prediction methodologies, understanding the parameters which controls the bubble size and their rate of oxidation and ozonation process are vital.

1.3 PRINCIPLE CONTRIBUTIONS

A novel method is proposed using machine learning approach to determine the values of the system operational parameters in generating a particular MNB size and to determine the MNB size range for effective removal of arsenic and coliform bacteria from water.

1.4 RESEARCH OBJECTIVES

1. To generate, determine the effect of size, stability and duration of MNB in water and to find out the optimum conditions for effective treatment.
2. To determine the efficiency of ozone MNB for removal of Arsenic and Coliform.
3. Development of a prototype for testing the real samples, automation for controlling and monitoring the size of MNB in the system.

1.5 THESIS OVERVIEW

A short overview of the chapters following this introduction is presented below.

- **Chapter 2:** This chapter discusses overview of different methods used to treat arsenic and coliform contaminated water. Advantages and limitations of the treatment approaches are studied to understand how oxidation rate helps in effective removal of arsenic and coliform from water. The possibilities of using MNBs of different sizes, their properties, generation methods and limitations are also discussed.
- **Chapter 3:** Here the complete experimental lab scale setup development is described including the materials and the methods necessary to carry out the study. Study was conducted to understand MNB size generation at different experimental conditions. Surfactants were also used for better understanding of MNB size reduction. The results achieved from the study were used as an insight in upcoming chapters.
- **Chapter 4:** This chapter describes a very brief overview on how humans get exposed to arsenic and coliform bacteria via water sources. Experiments were performed to test the oxidation capability of MNBs to convert As(III) to As(V) while in case of coliform, ozone gas was used to disinfect the cell wall. It was observed that smaller bubble size resulted in effective oxidation and disinfection.
- **Chapter 5:** The use of different machine learning models to explore the possibility in predicting MNB size is explored to provide a proof of concept. This approach was used as an alternative to high end sensory needs to understand MNB size generated. Two different modelling approaches (a) decision tree and (b) multi linear regression models were used to define relationships between different parameters of the system responsible in MNB generation.

CHAPTER 2 LITERATURE REVIEW

This chapter presents a brief review of literature, a summary of arsenic and coliform contaminations, their source of human contact, harmful disease and different methods for effective removal of arsenic and coliform from water sources. A brief about what are micro-nano bubble, their generation methods, properties and different applications is also presented.

2.1 ARSENIC CONTAMINATION

Over the years drinking water contamination caused by heavy metal ion such as Arsenic (As) have been a concern by several countries like India, Bangladesh, China, Nepal, Thailand, Brazil, United States, Canada, England relies on groundwater to meet the purpose of drinking[25]–[30]. Arsenic, a toxic element and widely distributed in our earth's crust is released into environments via groundwater. Most of arsenic problems in third-world countries today are caused by natural erosion. WHO estimated around 200 million people worldwide are exposed to arsenic contaminated drinking water which exceeds the recommended limit of 10µg/l given by WHO. India, it is estimated 20 million people consume arsenic contaminated water in different states West Bengal, Bihar, Uttar Pradesh and Punjab[31]–[35].

Primarily Arsenic is present as an oxy anion in groundwater representing two oxidation states arsenic As(III) (arsenite) and arsenic As(V) (arsenate) [36], [37]. At pH range of 2–12, predominant species of As(V) are H_2AsO_4^- or $\text{H}_2\text{AsO}_7^{4-}$. On the other hand, As(III) mainly exist as H_3AsO_3 at pH below 9 and H_2AsO_3^- is dominant at pH values of 9–12 [38] in. Compared to As(V), As(III) is more soluble resulting in increase of its mobility. Human exposure medium for As is shown Figure 2.1. Consumption of As at higher concentrations causes gastrointestinal problems and arsenicosis [39], [40] and the common symptoms include pigmentation, keratosis and skin cancer.

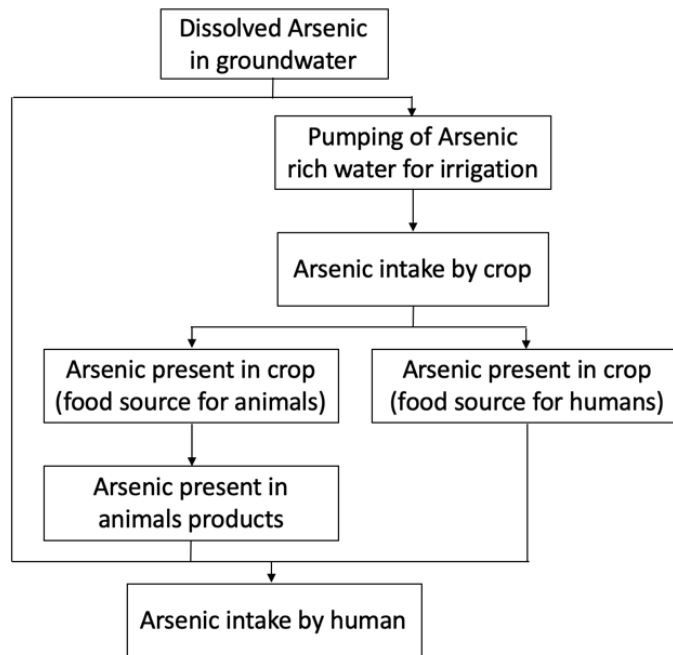


Figure 2.1 Arsenic Intake Medium by Humans [41]

2.1.1 ARSENIC REMOVAL METHODOLOGIES

There are several studies have been conducted on As removal methodologies over the past decades such as selective membrane methods[42], [43], reverse osmosis[44]–[46], adsorption[47]–[49] , oxidation, precipitation and various biological processes. These have their own advantages and disadvantages and most of the techniques adopt peroxidation method converting As(III) to As(V).

Coagulation flocculation method is a two step process in which at first chemicals are added to arsenic contaminated water in order to destabilize and convert the compounds into an insoluble precipitate[50]. This precipitate is used in the second step where it can be removed via sedimentation process or sometimes by filtration. Different chemicals are used as a coagulant which includes alum, iron, manganese, lime and electrocoagulation. Majority of the cases aluminum salts such as aluminum sulphate $[Al_2(SO_4)_3 \cdot 18H_2O]$ and ferric

salts such as ferric chloride $[\text{FeCl}_3]$ or ferric sulfate $[\text{Fe}_2(\text{SO}_4)_3]$ are commonly used in developing countries because of their low cost and relative ease of handling [15]. The effectiveness of iron coagulants in removing arsenic (III) diminishes at pH 6.0. The limitation of this method is the need of chemicals at different time intervals into the water producing a huge amount of sludge [51]. While in adsorption process, a solid medium for removing arsenic from water is used. Due to its high removal efficiency and ease of operation it is most widely used method. This method doesn't need any chemical substrate and is low cost sludge free process making it more feasible for use. Over the past, several different adsorbents such as metal based adsorbent, iron oxide, activated alumina and carbon based adsorbent have been used to adsorb arsenic from water[52]–[54].

Activated alumina and Iron-Based Sorbents (IBS) were the most widely used techniques for arsenic removal from drinking water. Even membrane based technology was used to test its feasibility of operation, these are made of synthetic materials containing billions of pores on them. These pores act as barriers and allows a part of water to pass through them leaving behind the waste present in water. This system requires a pressure medium to transport the water through the pores and are classified as low pressure and high-pressure process. Low pressure comprises of micro filtration and ultra-filtration whereas high pressure consist of nano filtration and reverse osmosis mediums. In both the cases, studies show's the need of an effective pre-oxidation of As (III) to As (V) for removal of As from water. Table 2.1 illustrates conventional and non-conventional methods for As removal.

Table 2.1 Arsenic Removal Methodologies from Water

Treatment Process	Type of Agent	Advantages	Drawbacks	Ref
Coagulation	Ferric Chloride	Ease of the process	Highly influenced by the type and dosage of coagulant, pH of the solution and availability of other competing anions, especially the iron content of the water sample.	[55]– [57]
	Ferric Sulphate	High stability of Fe-based coagulants over a wider range of pH having a high affinity for As compared to Al-based coagulants.	Producing As-contained sludge with high handling cost	
	Aluminum Sulphate		Not suitable and efficient for the removal of trivalent arsenic pre-oxidation may be needed	
Chemical oxidation	Hydrogen peroxide	Easy to be incorporated into existing treatment plant	High amounts of chemical agents required. Required pre-oxidation of As(III) to As(V) prior to coagulation, membrane filtration, and adsorption process.	[55], [58], [59]

Treatment Process	Type of Agent	Advantages	Drawbacks	Ref
Advanced oxidation processes	Photocatalysis (UV/TiO ₂ , UV/ZnO)	High oxidation rate	Only effective for the conversion of As (III) to As (V)	[58], [60]–[64]
	UV/H ₂ O ₂	No generation of toxic or hazardous intermediate by products during the conversion of the target pollutant	Non-selectivity of the treatment process	
Adsorption	Granular activated carbon (GAC)	High efficient for the removal of As (V)	Only transferring the target pollutant from one phase to another phase	[47], [65]
	Activated alumina		Need for the regeneration of spent adsorbent after four to five working run	
Ion-exchange	Natural and synthetic resins	High capacity for the sequestration	High operation and maintenance costs	[58], [66]

2.2 COLIFORM CONTAMINATION

Yet another global problem in drinking water is the presence of harmful microbiological pathogens. Water must be substantially free of dissolved salts, plant, animal waste and bacterial contamination to be suitable for human consumption. Presence of these substances in drinking water should be considered as a possible indication of microbiological activity and water quality deterioration. Nearly 5.7% of global diseases and 4% of global deaths are related to water, sanitation and hygiene (WASH) leading to 1.9 billion people worldwide consuming water from unimproved/improved sources of water that is fecal contaminated and mostly supplied through rural piped or groundwater sources [67].

Reportedly 37.7 million Indians are affected by waterborne diseases. Most of these microbiological contaminations is observed in lower and middle income countries with fecal contamination being most predominant in South Asia and Africa [68]. Since 2017, diseases such as cholera, acute diarrheal, viral hepatitis and typhoid have caused 10,738 deaths [67].

Coliforms contain a thin peptidoglycan layer making it a gram negative bacteria and are also oxidase-negative, non-spore forming rods which ferment lactose with gas production at 35–37 °C, after 48h, in a medium [69]–[71] and are capable to survive with a very little or no oxygen by using anaerobic respiration. Composition of the coliform group is illustrated in fig.2.2.

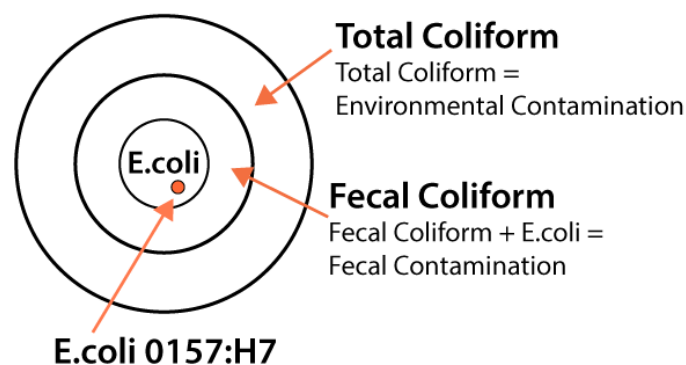


Figure 2.2 Classification of Coliform Bacteria

The elderly, children, pregnant women and immunocompromised persons are more prone to water borne illness. In developing nations like India, where groundwater is the primary source of for irrigation, industrial needs and drinking purposes. It is estimated that more than 90 percent of groundwater is used for irrigation and the rest is used as source for drinking water.

Other sources of water include rainwater harvesting and the network of major and minor canals originating from Indian rivers. Governments, farmers and local municipalities of India rely on major river sources of India such as Ganga, Yamuna, Kaveri, Sabarmati, Krishna and Godavari to meet their water demand. But with release of industrial pollutants, sewage originate from domestic and agricultural waste are discharged into these rivers has made the water unsafe [72]–[75].

Studies have shown that *E. coli* survival on soil medium is relatively possible given to the soil texture and physicochemical properties [76]–[78]. Major parameters for its long survival stint is due to the presence of Soil Organic Carbon (SOC) and organic nitrogen in in organically manured soils. Irrigation of agriculture using contaminated water or in soil has resulted to the bacterial presence in the vegetables [79], [80]. Sources of possible contamination and how does coliform bacteria enter into our digestive system is illustrated in fig.2.3.

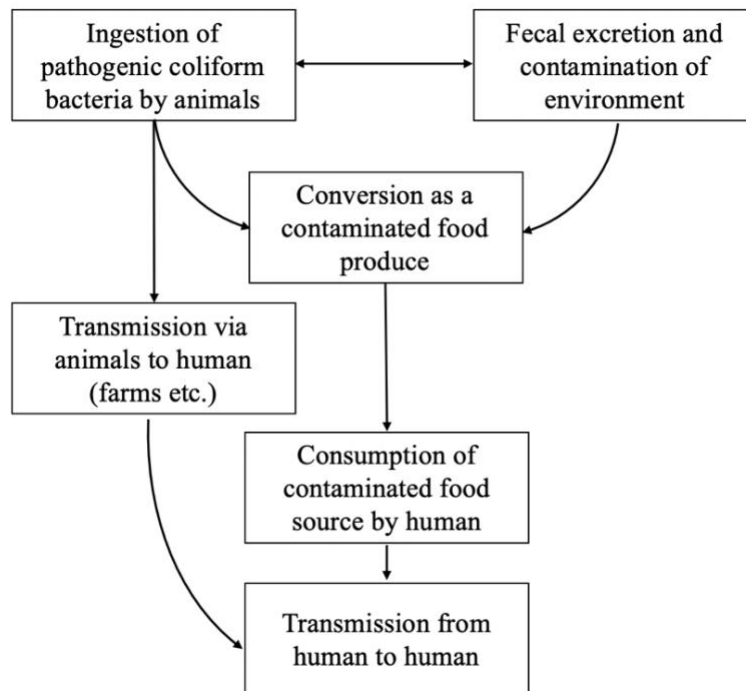


Figure 2.3 Process of Coliform Bacteria Intake by Humans

2.2.1 COLIFORM REMOVAL METHODOLOGIES

Over the decade chlorination, iodination and ultraviolet light are the popular methods used as a disinfection method in water treatment. Due to their limitations to form byproduct residues that are undesirable and harmful in nature of chlorine, few countries have started to ban the use of such chemical disinfectants which led to an increase in research study towards other disinfection processes such as ozonation, membrane and nano particles. Li Guo et al [81] demonstrated a process to combat the environmental viruses using cold atmospheric-pressure plasma and plasma-activated water where they used surface plasma in argon mixed with 1% air and plasma-activated water was used to treat water containing bacteriophages. However, this process is yet to be tested for large scale application given to its high-power consumption capacity for its electrodes. Use of metal oxides have also been tested for its antibacterial properties to govern photocatalytic activity against *E. coli*. Findings of studies have also shown to improve photocatalytic efficiency, such as increased amount

of Reactive Oxygen Species (ROS), specific light spectrum and intensity, and particles morphology [82]. This technique is based on the principle of photo-excitation of a semiconductor oxide upon absorption of light radiation where electrons present in the valence band (VB) of semiconductor such as zinc oxide (ZnO), tungsten oxide (WO₃), titanium oxide (TiO₂) etc., are excited to the conduction band (CB), leaving a positive hole in the valence band [83]. Formation of electrons and holes in this process implicate redox reactions.

Disinfection mechanisms using solar is also tested for its efficiency towards microbes, but this method is limited to implementations to large scale applications. While with the use of Atmospheric-pressure low-temperature plasma (APLTP), the cell morphology of E.coli was changed leading to the rupture of cell wall, membrane and losing the ability to reproduce[84]. The SEM images of E.coli before and after treatment by APLTP is shown in the fig.2.4.

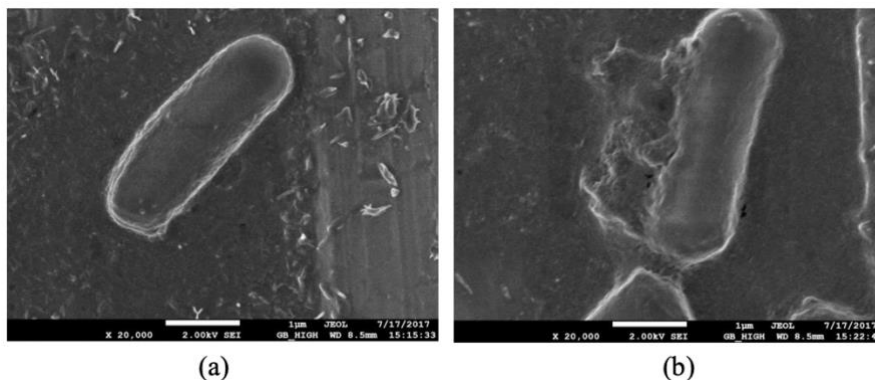


Figure 2.4 Scanning Electron Microscopy (SEM) images of E.coli; (a) Controlled E.coli; (b) Treated E.coli [84]

To control the contamination of water sources one way is by treating the contaminated water emerging from industries prior releasing it to the water streams. Such a process requires large build area and huge capacity for treatment process is required. Disinfection process via ozone has gained attention for addressing the situation. Ozone is known for its most efficient in wastewater disinfection and decontamination procedures[85]–[87].

2.3 MICRO-NANO BUBBLE (MNB) IN WATER TREATMENT

With an increase in water pollution levels due to chemical, physical and biological contaminations emerging in water bodies from different sources such as industrial wastes, farm lands, household, waste dumping's near water sources etc., have raised concerns for water treatment methods towards safe drinking. Over the decade, several studies have been implemented to treat water but with an increase in pollutants, researchers are more inclined towards treatment methodologies which are environmentally friendly, cost and energy efficient.

Micro-Nano Bubble (MNB) are tiny small bubbles with diameter ranging in micro and nanometers [88]–[90]. These bubbles have drawn attention of several researchers over the past years for its potential in water treatment industry. Bubbles of different sizes have been implemented in different applications such as medical, agriculture, aquaculture, sterilization and cleaning, removal of contaminants and heavy metals from water [91]–[93] . Compared to conventional bubbles, with diameters of up to several millimeters, MNBs have huge interfacial areas and greater bubble densities. Microbubbles also have a low rising velocity in the liquid phase and a high inner pressure [94]. Due to these unique properties, microbubbles have found their place in various research areas.

MNBs constitute of three components, a gas phase (specific or mixture of different gases), shell (solution surrounding the gas phase) and medium (aqueous/ air) where a bubble is generated as shown in fig.2.5.

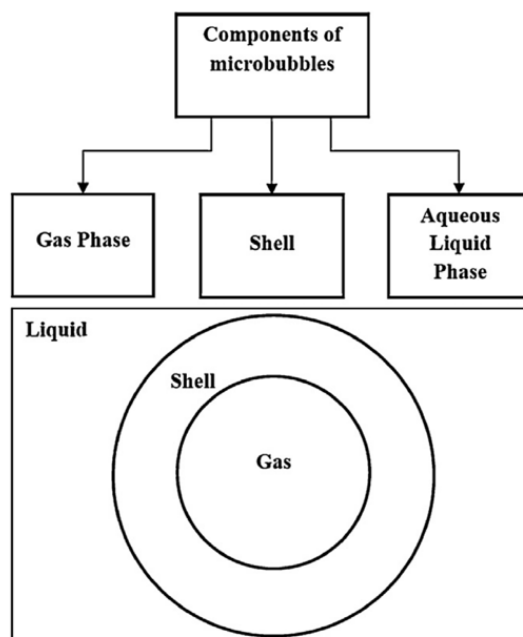


Figure 2.5 Structure of a Micro-Nano Bubble (MNB)

Gas Phase:

The gas phase comprises of a single gas or combination of gases. Applications where a combination of gases are needed is generally to create differentials in partial pressure and in sometimes it is also used to generate gas osmotic pressures which help to stabilize the bubbles. In such instances one gas is called primary gas modifier or first gas while the second gas is known as gas osmotic agent. Gas which is less permeable through the bubble surface than the modifier is preferred as gas osmotic agent. Nitrogen and air are examples of primary modifier gas, sulfur hexafluoride is an example of osmotic gas agent.

Shell Material:

The shell material encloses the gas phase. This material is responsible for effective diffusion of gas out of microbubbles and plays a vital role in encapsulation of drug molecules for medicinal applications. If the elasticity of shell material is more, the acoustic energy it can withstand before bursting or breakup is high, which increase the residence time of the bubbles.

Liquid Phase:

The external liquid in which bubble is generated surrounding the shell can be same as of shell material, or it can be surfactant or foaming agent depending upon the operational/application conditions.

2.3.1 PROPERTIES OF MICRO-NANO BUBBLE (MNB)**2.3.1.1 SIZE AND SHAPE**

Micro-nano bubbles are spherical in shape having the diameter in the range of 10nm to 10 μ m. This results in minimal gas liquid interfacial energy. Several studies have given different names for example in the study on physiological activity microbubbles are considered to those having bubble diameter in the range 10–40 μ m whereas in the field of fluid physics the bubbles with diameter of about few hundred micro meters or less is considered as microbubbles. Ohnari [95] defined microbubbles as bubble with diameter in the range of few hundred nm to 10 μ m, and nanobubbles to those bubbles which are having diameter less than few hundred nm. While bubbles in millimeter and larger are termed as macro bubbles and bubbles whose diameter is between 200nm to 10 μ m are termed as micro-nano bubbles. Fig.2.6. shows the key differences among different bubbles, as illustrated it can be observed that bubbles of larger diameter tend to rise to the surface faster and burst, however bubbles with smaller diameter gradually decreases its size and collapse due to dissolution of gases while bubbles which are very tiny sized tends to stay longer.

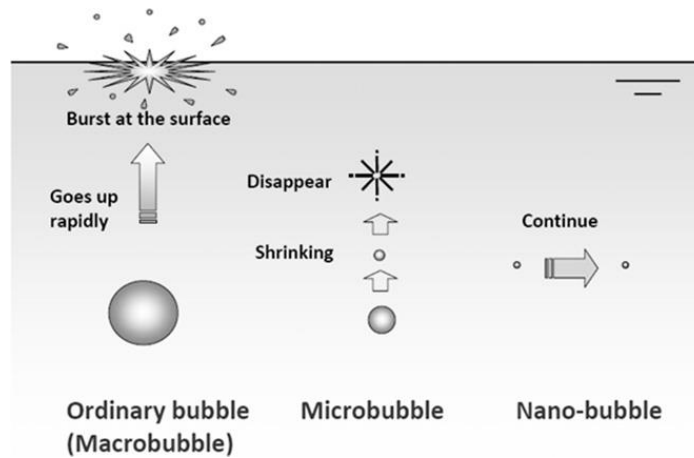


Figure 2.6 Diagram showing macro, micro and nanobubbles[96]

2.3.1.2 RESIDENCE TIME

The physical properties of liquid affect the rising speed of microbubbles. Reynolds number for microbubbles is very less (approximately $Re \leq 1$), due to its small size. The bubble motion is greatly influenced by Brownian motion between the bubble and the surface, as well as Van der Waals force. The theory is about the random motion of small particles that immerse in a fluid medium. Rise of temperature surrounds the particle can affect the Brownian motion. If the equivalent radius of bubble is smaller than $100\mu\text{m}$, the shape of bubble remains almost spherical and the bubble behaves like solid sphere, if the equivalent radius increases, a change in bubble shape from spherical to ellipsoidal to spherical cap can occur.

The radius at which these transitions occur depends on the physiochemical properties of the liquid. When the size of bubble reaches to micron level, i.e. Reynolds number approaches to zero, bubbles can be considered as rigid spherical body. Thus the terminal rise velocity of microbubble can be described by Stokes' law [97], where the terminal rise velocity of the bubble in a viscous liquid at low Reynolds number is expressed in Eq. 2.1.

$$U_b = \frac{D_b^2(\rho_l - \rho_g)}{18\mu_l} \quad (2.1)$$

2.3.1.3 SELF-PRESSURIZING EFFECT AND RISE TIME

The most significant property of microbubbles is its decreasing in size under water, and the surface tension increasing the pressure inside the bubble inversely proportional to the bubble's diameter. The relationship between pressure and diameter is expressed by the Young-Laplace equation as illustrated in fig.2.7. However, high Laplace pressure inside NBs would likely cause them to dissolve into solution quickly [98]

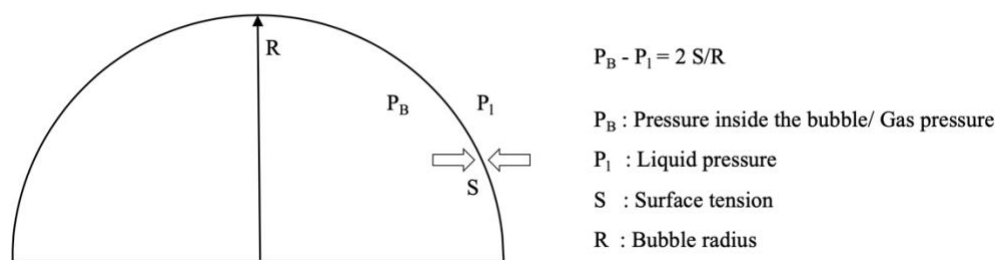


Figure 2.7 Young laplace law [99]

2.3.2 GENERATION OF MNB

Different MNB generation methods [100] are as follows.

2.3.2.1 ROTARY LIQUID FLOW TYPE

Water is first pressurized and is pumped tangentially from a side hole into a cylinder as shown in fig.2.8. This produces a spiral/rotary flow inside forming a cavity and causing a reduction in pressure in its central axial part. The required gas is introduced from an orifice and this comes out through the other end of the cylinder mixing effectively due to the centrifugal effect caused by pressurized water thereby forming microbubbles.

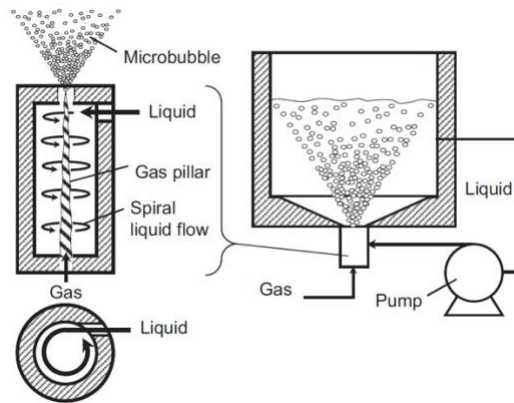


Figure 2.8 Rotary liquid flow type MNB generator

2.3.2.2 VENTURI TYPE

This method is similar to rotary flow to a certain extent. Here both the gas and the liquid are introduced from the same end of the device as shown in figure. As it can be seen, the throat of the venturi accelerates two phase fluid i.e., the gas and the liquid. Pressurized fluid is sent and due to the pressure created at the throat section a decrease in pressure creates cavitation in the system resulting in micro-nano bubble formation. Through this method a 100 μm sized bubbles were generated by Fujiwara [101].

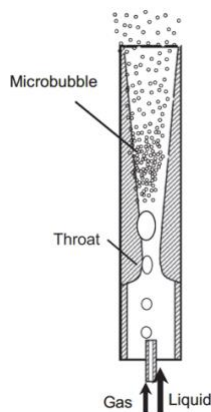


Figure 2.9 A venturi type MNB generator

2.3.2.3 PRESSURIZED DISSOLUTION TYPE

Schematic of this method is shown in figure. In this method, air is mixed with water through a pressure of 3-4 atm. Pressure of the system is controlled using the valves present at suction and discharge end of the pump. Presence of reduction in pressure in the pump head, supersaturated air is released into expelled water which forms microbubbles. The discharge valve helps to control the size and population of the micro-nano bubbles being produced.

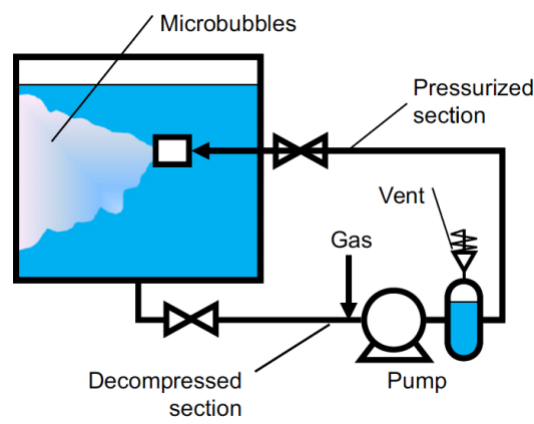


Figure 2.10 MNB generation through pressurized dissolution method

2.3.2.4 EJECTOR TYPE

This process uses venturi effect to convert pressure energy of the fluid to a velocity energy creating a low pressure zone drawing in the suction gas via a converging-diverging nozzle. The liquid-gas mixture expands and its velocity is reduced once it has passed through the throat of the injector. Microbubbles of 40-50 μ m can be generated via this process.

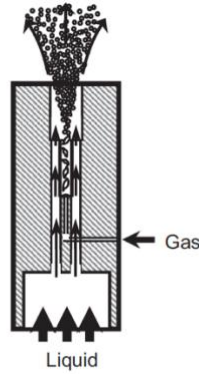


Figure 2.11 Ejector type MNB generator

2.3.2 MICRO-NANO BUBBLE SIZE DETERMINATION

Few studies have also shown the use of image processing techniques to determine the size of MNB. This method requires a high-resolution camera and macro lenses. The camera should be able to capture images with at least 19 frames per second which enables to identify the best captured image for analysis using software's on a computer. However, it was observed that the minimum measurable size through this medium was estimated to be $0.8\mu\text{m}$. This being the reason particle size analyzer method was most widely used given to its size measuring capacity from to 10nm to $100\mu\text{m}$. This method uses laser diffraction and is determined according to the dispersal coefficient (δ) of particle size as given in Eq.2.2.

$$\delta = \frac{D_b^{90} - D_b^{10}}{D_b^{50}} \quad (2.2)$$

Where D_b^{10} , D_b^{50} and D_b^{90} are the diameters corresponding to 90,50 and 10% by volume respectively, on the relative cumulative bubble size distribution curve.

Specific interfacial area of micro-nano bubbles is defined in Eq. 2.3

$$a = \frac{6\varepsilon_G}{D_b^{50}} \quad (2.3)$$

Where ε_G is

$$6\varepsilon_G = \frac{V_g}{V_L + V_g} \quad (2.4)$$

ε_G is gas hold up, V_g is the gas phase volume and V_L is the volume occupied by the liquid phase. Takahashi, M [102] pointed out that the rising velocity of microbubbles bigger than 7–8 μm approximately obeyed the Stokes' law, while bubbles smaller than 7–8 μm rose more slowly than calculated.

2.3.3 APPLICATIONS OF MICRO-NANO BUBBLE

Hengzhen Li et al [103] demonstrated that MNBs ranging from 500 nm to 100 nm were capable to enhance dissolved oxygen level facilitating aerobic biodegradation process for applications such as groundwater treatments. They also studied the effects of surfactants on MNBs. Results showed that though they were capable to reduce the bubble size but it also reduced the oxygen transfer efficiency. While another study [104] reported the growth of biofilm using nanobubbles. The investigation was to understand and determine the contaminant removal ability of the biofilm and the internal oxygen supply to biofilm using nanobubbles and coarse bubble aeration. Yanmei Sun et al demonstrated the combination of MNB with submerged resin floating bed composite technology for treating stinking urban river water [105]. This method significantly improved the river water quality such as dissolved oxygen, ammonia nitrogen, total phosphorus, coliform, water clarity and chemical oxygen demand.

Oxidation of AS (III) to AS(V) was observed by Khutia et al. in a pilot scale setup. Using 30 μm ozone microbubble resulted in effective oxidation with an increase on ozonation rate [106]. It was also noted that the conversion factor was more affective a pH 6 than compared to pH 7. M.D. Sharifuzzaman et al observed the efficiency of MNB in a pretreatment process for removing fluoride from wastewater emerging from an industry [107]. A study performed for 56 days of shrimp culture period resulted in increase in survival rate to 92% using nanobubbles while compared to normal shrimp pond with a survival rate of

75%. This was only due to proper distribution of dissolved oxygen thorough out the pond achived by nano bubbles [108]. Use of MNBs have also been implemented in floatation process, where bubble size and its distribution were the major factors which affected the fluid behavior of the flotation column. Parameters like rate of aeration, circulating pressure and frother consumption are important for the formation of air bubbles. Use of surfactants can help in reducing surface tension and increase bubble stability. Though the froth generated can be beneficial towards effective oil water separation but can introduce other secondary pollutants which might need attention while treatment process. Few other potential applications of MNB are described in Table2.2. These applications shows a cost effectiveness approach of MNB given to their less dependencies on chemicals and their dosage rate. Few cases the need of chemicals can be avoided such as in water treatment, chlorine can be replaced with ozone gas for effective disinfectant of portable water. Such mediums make this MNB technology more cost effective and environmental friendly.

Table 2.2 Applications of MNB

Application	Remarks	Bubble Size
Agricultural Use	Yaxin et al [109] showed the use of MNB for tomato and cucumber cultivation which resulted in increase in their yield and fruit quality without any increase of fertilizer and other substances. MNB also resulted in reduced water use.	163 nm ± 12 nm
	Huaming Hg et al [110] study showed the use of ozonated micro-nano bubble water for preventing tomato airborne disease.	5-30 nm
	A study by Honghui Sang et al [111] showed that micro-nano bubble based aerated irrigation and nitrogen fertilizer had a substantial influence on tillering of early rice and the effect of N fertilizer was greater than the effect of oxygen.	700nm- 12µm
Water and wastewater treatment	Based on the initial findings suggested by Sumikura et al [112], by use of ozone micro-nano bubbles towards disinfection of secondary effluent there is a possibility to reduce the reactor size and ozone dosage rate.	30-40µm

	<p>Deessiree Menendez et al [113], utilized ozone-air micro-nano bubbles to treat hospital waste water resulting in decrease of concentrations of BOD5, COD and TSS within 15 mins of treatment time.</p> <p>Silva et al [114]demonstrated a pilot scale setup to treat raw water for calcium and magnesium prior using it in steam generator was studies in a pilot scale using micro-nano bubbles.</p>	<p>0.024µm</p> <p>100-500nm</p>
Aquaculture	<p>Study conducted by Asri Ifani Rahmawati et al.[115], showed promising results for an increase on productivity of shrimp farming. It was observed that the total harvest and productivity was doubled to 436 kg and 8.7 kg/m3. Nanobubble was capable to manage and maintain DO at the required optimal range and affected shrimp growth significantly.</p> <p>A similar study conducted for Tilapia fish showed that air bubbles were capable to increase the daily growth rate. In addition, bubbles were also able to increase the flotation of uneaten food, feaces, which were responsible for increase in turbidity in water and helped to decrease the ammonia toxicity [116].</p>	<p>82.93 nm</p> <p>14µm</p>

As the studies showed that MNBs have their potential in different applications, but it is to be noted that the size of MNBs in all the applications is not constant. Majority of the studies in this field being at a laboratory scale, implementation of such system at a larger scale brings a limitation of size determination due to lack of sensing ability of the sensors at such nano scale in an automated system. Moreover, presence of any debris or minute dust particles can also hamper the sensing ability by mistaking it to a MNB. Therefore, need of technological interventions for MNB size determination still remains a thrust are for several researchers.

One such methodology is the use of Machine Learning algorithms to predict the size of MNB with the help of data analysis of the database containing different system operating parameters and their respective MNB size.

Data analysis is extensively used to design models for facilitating prediction that provides better understanding of a large dataset. Prediction method is a form of data analysis that can be used by both human environmental scientists and computer-aided Environmental Decision Support Systems. Predictive tasks facilitate safety operations. With the help of data-driven approach, the treatment process can be more accurately represented using models without the need of solving complex physical and mathematical equations. The models can also be used to predict the behavior of the plant and be solved with evolutionary algorithms to find the optimal control settings to save energy and improve efficiency of the system.

CHAPTER 3 MICRO-NANO BUBBLE (MNB) GENERATION

This chapter presents the study carried out on Micro-Nano Bubbles(MNB), their generation method, size determination and stability. Based on the literature survey, MNBs were generated via pressurized dissolution methodology. They were further tested for their existence and size characteristics at different temperatures using different gases.

3.1 EXPERIMENTAL SETUP

A laboratory scale pilot plant setup for MNB generation was designed and developed based on pressurized dissolution method as illustrated in figure 3.1. Pressurized dissolution methodology was used to generate MNBs. Since most of the applications of MNB is towards water treatment and other similar applications, it was observed that gases such as compressed air, O₂ and O₃ were most widely used for water treatment, potable water disinfection, dissolved air floatation, increasing D.O. levels in aquaculture etc., therefore these three gas mediums were considered for their performance evaluation. Prior experimentations, the complete setup was cleaned with distilled water to avoid presence of any tiny particle which could obstruct MNB detection.

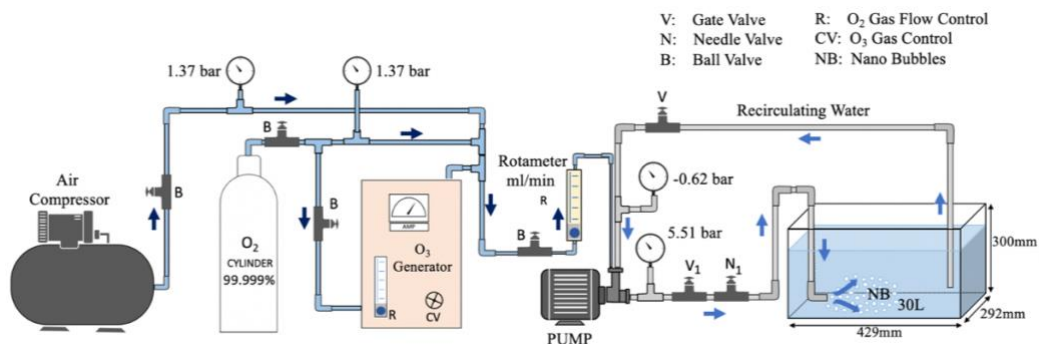


Figure 3.1 Schematic diagram of experimental setup

MNBs were generated using a multiphase centrifugal pump (Nikuni KTM 20) paired with a needle valve (Parker, N800,1/2”) was used to generate bubbles in a glass tank of 30L capacity. O₂ gas was used to produce 5% of O₃ gas concentration. Rexroth Bosch (Brilliant 50-16) was used to generate compressed air.

3.2 MEASUREMENT OF MNB SIZE

MNBs when produced, generates a milky white solution flow due to the presence of dense tiny bubbles. Owing to its density, measuring methods such as image processing, use of optical microscope isn't followed due the complexity. Dynamic light scattering technique was adopted where a particle size is determined/measured in microseconds by measuring the random change in the intensity of the light scattered by the suspension. In this technique, diffusion is measured by measuring the fluctuation intensity of the scattered light produced by the particles which are diffusing due to their Brownian motion. Therefore, smaller the particle the more the fluctuation intensity.

Hence, Particle Size Analyzer (PSA) (N90S, Malvern) was used to determine the size of MNB. Throughout the experimentations, a sample size of 10 ml was taken in a quartz cuvette (SIGMA) and was placed inside the PSA for analysis. Each sample analysis contained one measurement cycle comprising of sample equilibration time of 30 secs followed by size determination for four different runs of 20 secs each. The size of the MNB is expressed as Z_{avg} .

Z_{avg} can be expressed as

$$Z_{AVG} = \frac{\sum S_i}{\sum \left(\frac{S_i}{D_i}\right)} \quad (3.1)$$

Where S_i , is the scattered intensity from particle (i) and D_i is the diameter of the particle.

3.3 EXPERIMENTAL PROCEDURE GENERATION

3.3.1 MNB GENERATION

The experimental test bench is shown in figure 3.2 operated in recirculation mode throughout the experiments. Distilled water which is pure from presence of any solid particles was used as a liquid media for bubble generation. This media helped to avoid mis interpretation of bubble size in PSA. Rotameters and ball valve were used to regulate the flow rate of the feed gas and the pressure of the liquid flowing through the pump. Following is a step by step process method applied for generating Micro-Nano Bubble through pressurized dissolution method.

Step 1: The complete setup was run with 3L of distilled water for a duration of 10 mins. This helped in efficient circulation of water and removal of any particulate matter present in the system.

Step 2: The circulated water was removed from the setup and was thoroughly cleaned prior filling the tank with 10L of distilled water

Step 3: Setup was turned on for a duration of 5 mins, which enabled the user for setting the necessary experimental parameters responsible to generate the bubbles.

Step 4: After setting the required parameters, the system was shut off for a duration of 10 mins, which allowed for the primary bubbles generated during setting the parameters disperses.

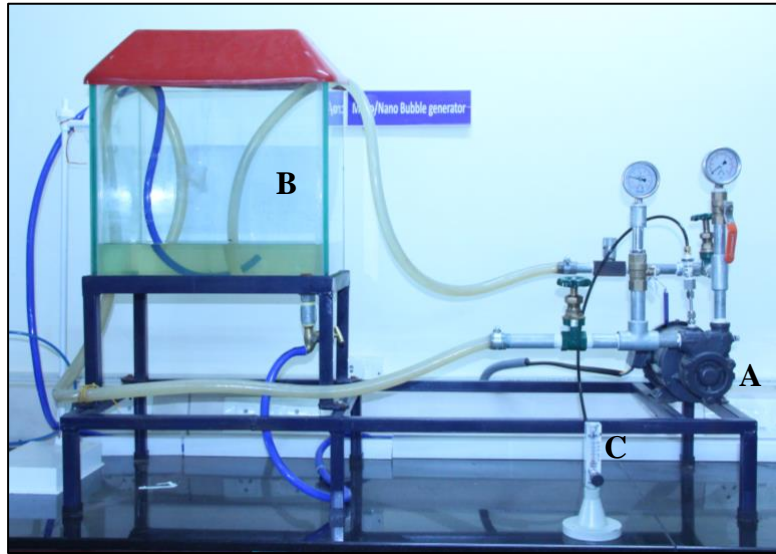


Figure 3.2 Experimental setup; (a) Micro-nano bubble generator; (b) Water tank; (c) Rotameter

3.3.2 EXPERIMENTAL CONDITIONS

The bubble generator, working on the principle of multiphase centrifugal enables to work at different pressure conditions which helps to generate bubbles at different sizes. To further better understandings of bubble size, the parameters prompting bubble size to change were tested as described in table 3.1. As the objective of the study is to understand and predict the size of MNB, understanding the role of these parameters are very essential.

Table 3.1 Experimental Parameters

Parameter	Value
Input pump pressure	-9 psi
Feed gas rate	30 ml/min
Feed gas pressure	1.3 bar
Feed gas type	Compressed Air
	Oxygen
	Ozone
Water type	Distilled water
Volume of water	10 L
Inner dimension of tank	42.9L X 29.2W
No. of Runs per experiment	10
Bubble generation time	5 mins
Output Operational Pressure	60 psi

	80 psi
Operating Temperature	20°C, 25°C, 30°C, 35°C

From figure 3.3, it can be observed that MNBs when generated produces a dense cloud of bubbles thereby transforming the liquid into a milky white solution. The intensity of the solution reduces gradually with MNB rise time.

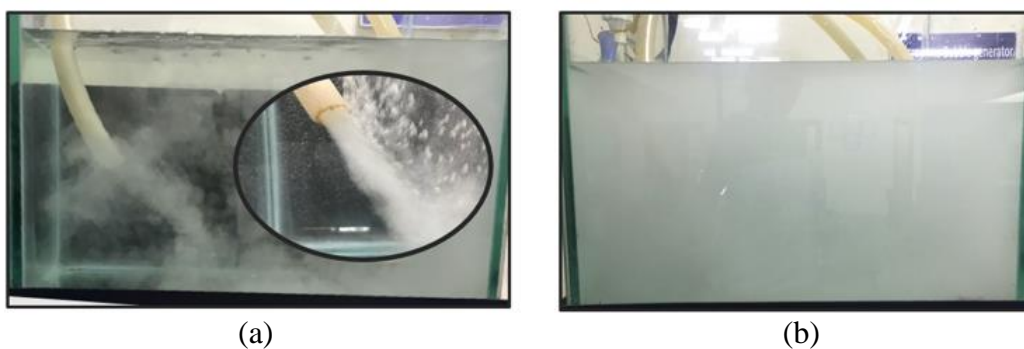


Figure 3.3 MNB generation; (a) immediately after starting the system; (b) after 5 mins of MNB generation

Throughout the experimentation, the bubbles were generated for 5 mins and later the system was shut off for monitoring the rise time of the bubbles. After MNB generation (5min) a sample was immediately transferred for its size estimation in PSA.

Initial experimentations showed that bubbles generated in distilled water were not stable due to lack of potential/charge on their surface area. These bubbles gradually increased their size by agglomerating with other bubbles which also lead to faster rise time to the surface. Hence to further understand their stability, two different surfactants were also used.

Presence of surfactants in water, reduces the surface tension and improves the efficiency of different processes. They contain a hydrophobic and hydrophilic parts are present in tail like structure over the surface of the bubble as shown in figure 3.4.

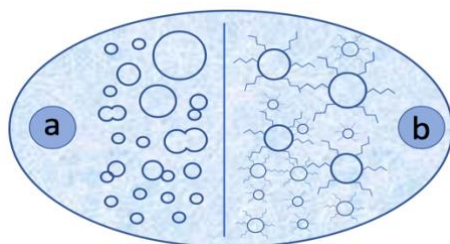


Figure 3.4 Structure of MNB; (a) in absence of surfactant; (b) in presence of surfactant

Addition of surfactants helps bubbles to retain their size for longer durations and avoid amalgamation of bubbles. Bubbles formed in the absence of surfactants showed less stability as they tend to rise to the surface faster. They also merge with fellow bubbles and increase in size. Addition of surfactants not only provides better stability but they also tend to break down the interface between water and oil/dirt.

As a result, surfactants are widely used as wetting agents, detergents and emulsifying agents. Closely packed MNBs surrounded by surfactant have electrostatic repulsion between the cationic and anionic ions on the surface of adjacent bubble, breaking down the interface between the water and other contaminants (oil and dirt) resulting their increase in range of applicability as wetting agents, detergents and emulsifying agents. Characteristics of different liquid media in which bubbles were generated is described in table 3.2.

Table 3.2 Composition of different surfactants used

Aqueous Solutions	Viscosity
Sodium Dodecyl Sulfate (SDS) Quantity: 100 ppm Molecular Formula: $\text{NaC}_{12}\text{H}_{25}\text{SO}_4$ Chemical Structure: $\text{NaO}-\overset{\text{O}}{\parallel}{\text{S}}-\text{OCH}_2(\text{CH}_2)_{10}\text{CH}_3$	2.17cP

Aqueous Solutions	Viscosity
Cetyltrimethyl Ammonium Bromide (CTAB) Quantity: 100 ppm Molecular Formula: $C_{19}H_{42}BrN$ Chemical Structure: $ \begin{array}{c} H_3C \\ \\ (CH_2)_{15} - N^+ - CH_3 \\ \\ CH_3 \end{array} $	2.17cP

3.3.3 EXPERIMENTAL RESULTS

Initial experimentations were carried at different system output pressure. It was observed that at an output pressure 40 psi and 50 psi the bubbles ranged in a much larger size and therefore the pressure was further increased. It was observed that at an operating pressure of 60 psi, the bubble ranged in micrometers from 1.1 μ m to 4 μ m in size shown in figure 3.5. Several studies have shown that bubbles ranging at this size were capable of removing toxic metal ions, dye stuff etc. Further O₃ bubbles could be used as an alternative disinfectant for removal of bacterial contaminates from swimming pool instead of using chlorine.

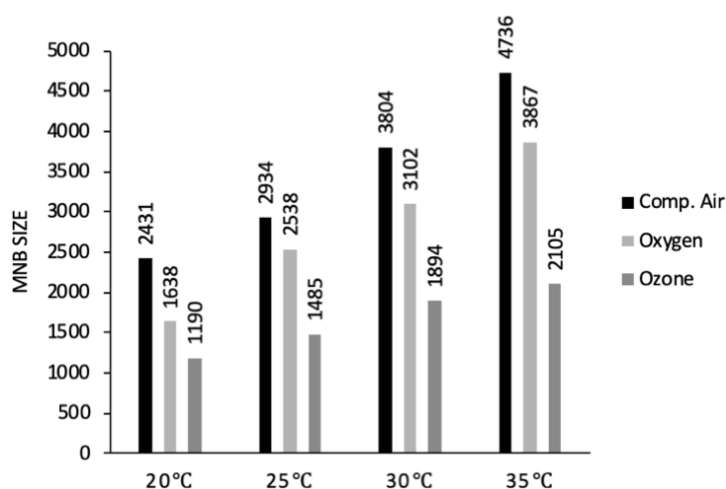


Figure 3.5 MNBs at 60 PSI

While conducting experiments at 80psi reduction in bubble size ranging from 809 nm to 4 μ m shown in figure 3.6. Bubbles of this size can be of a potential use in applications where longer residual and oxidation is necessary. Studies shows that nanobubbles are electrically charged at neutral pH [117] while the zeta potential for air nanobubbles were in the range of -17 to -20 mV (pH 5.7–6.2) and about -34 to -45 mV (pH 6.2–6.4) in the case of oxygen nanobubbles. It shows that zeta potential of bubbles are generally negative and is varied depending on the type of gas being introduced. This could be explained by the presence of excess hydroxyl ions (OH^-) relative to hydrogen ions. (H^+) at the gas–water interface in pure water [118]. Studies with MNBs in nanometer range have resulted in greater removal efficiencies.

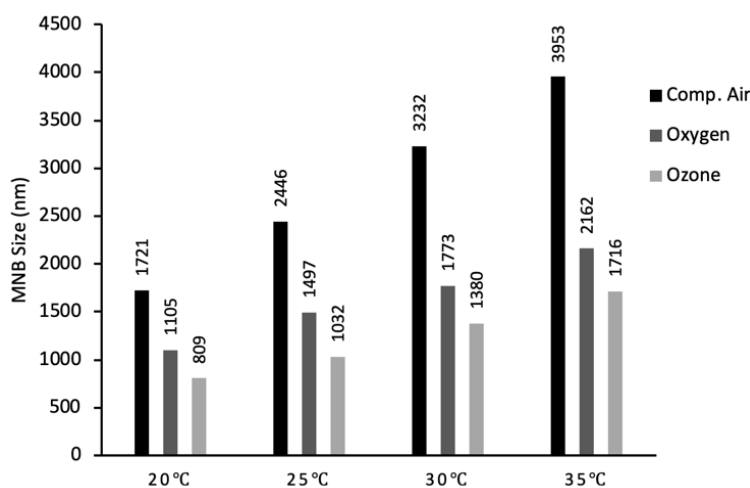


Figure 3.6 MNBs at 80 PSI

Therefore, further experimentations were carried out in the presence of surfactants, to understand bubble stability in water. A study conducted by Ushikubo et al. [119] shows that bubbles with a zeta potential >30 mV were much more stable than those with <30 mV. It was suggested that the stability of nanobubbles is mainly due to the magnification of electrostatic repulsive forces caused by overlapping electrical double layers of the neighboring bubbles.

Lifetime of the bubbles generated were studied by examining the change in bubble size present in the cuvette in DLS for a duration of 30min reported as x_f , while x_i is the size of bubble reported immediately after generation. During

experimentation, in absence of surfactants, it was observed that the bubbles generated using compressed air resulted in micrometers as shown in figure 3.7. This can be due to amalgamation of bubbles and lack of anionic or cationic agents on its surface to help it retain its size for longer duration. The impact of temperature was not clearly visible in CTAB compared to SDS. This is mainly attributed to the presence of long chain in CTAB that may help in reduction of surface tension, improving the size and stability. Here it should be noted that the stability of bubbles is governed by the balance between the roles of surface tension, surface activity and adsorption kinetics, where the smaller length of hydrophobic chain of surfactant molecule can increase the adsorption rate.

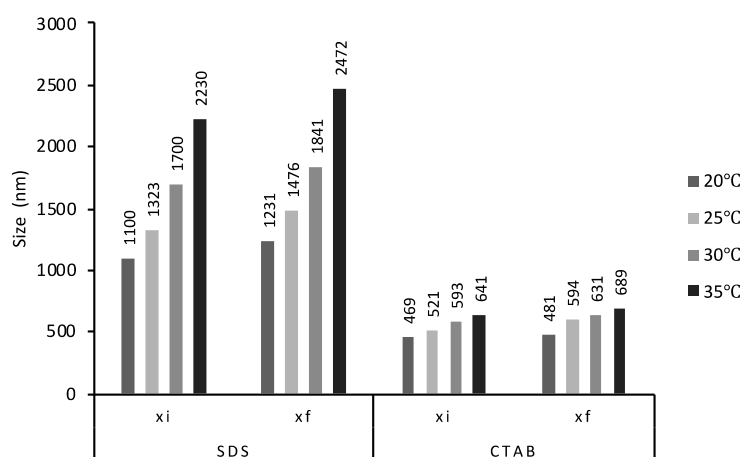
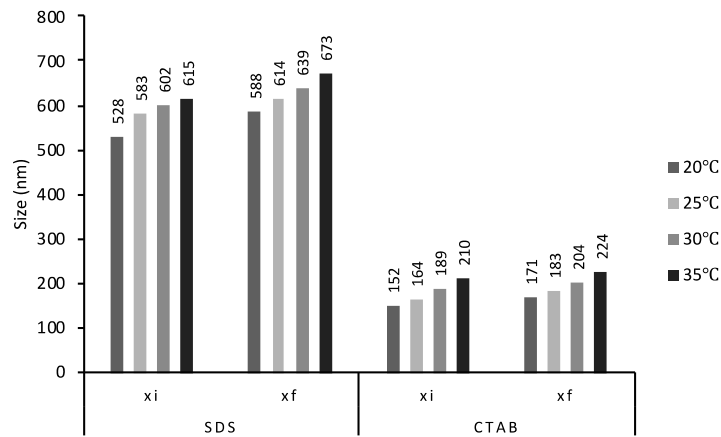
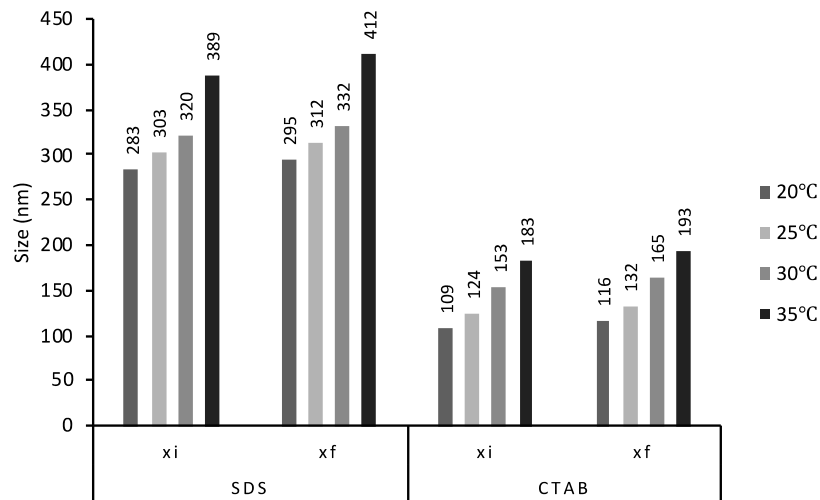


Figure 3.7 Compressed air MNBs in presence of surfactants

While from figure 3.8, shows that bubbles generated with oxygen gas and ozone gas respectively has reduced its size when compared to the bubbles generated through compressed air. These types of bubbles can be used in medical applications for tissue hypoxia and also in aquaculture and agriculture to promote the growth of plants and fishes. Studies shows bubble size in micrometer range are used in various applications of water treatment methods like dissolved air floatation methods, sludge solubilization process and also for separation of oil/dirt[120]–[123].



(a)



(b)

Figure 3.8 Stability of MNB in presence of surfactants; (a) Oxygen MNB; (b) Ozone MNB

Further, smaller size of MNBs in presence of CTAB (124nm) than SDS (303nm) just after formation of nanobubble was in contradiction of previous report [124], where it was shown that CTAB produced the largest bubble than SDS in presence of Polyoxyethylene Glycol 40 stearate in Tween 40 solution. It should be noted that all the experiments were conducted in low volume (30ml) at lab scale and bubbles size were mainly attributed to the wettability of channels by the surfactant molecule.

Most of the studies on stability and size of MNBs are surveyed at low volume[125], presenting stability for many hours ranging from 48 hrs to 150 days. Since the present approach was focused on developing a system for real time applications not only on smaller scale but also in large scale for water treatment. The time for size estimation was limited to 30 min due to distortion in the DLS results caused by the formation of large bubbles on cuvette shown in fig. Hence to further observe existence of MNBs scattering of laser beam method was used to determine their presence which were observed till 60 mins after generation[125].

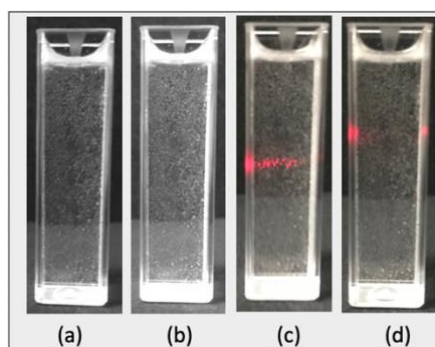


Figure 3.9 Observation of lifetime of MNBs in a 5ml cuvette; (a) at time $t= 15\text{min}$; (b) $t= 30\text{min}$; (c) $t= 45\text{min}$; (d) $t= 60\text{ min}$

It has been reported that ozonated water has a half-life of about 20 min and degrade back into oxygen. At different temperature regions, it can be seen from table 3.3 the rate of increase in size of a MNB in presence of CTAB is relatively slow when compared to SDS.

Table 3.3 Rate of change in MNB size after generation

Temp	SDS (% Increase)	CTAB (% Increase)
20°C	6.03	4.07
25°C	6.06	2.88
30°C	7.27	3.61
35°C	5.18	5.58

3.4 SUMMARY

It was observed that size of a MNB generated via pressurized decompression methodology depends on system operating pressure and the temperature of the water. Gas being used at the time of has the major role in reducing the size of a MNB. Use of surfactants such as SDS and CTAB effectively showed their impact on the size reduction and longer stability of MNBs although use of such surfactants is subject to further contaminations and require attention for their removal mechanisms.

CHAPTER 4

REMOVAL OF ARSENIC AND COLIFORM

This chapter illustrates the removal methodology adopted for eliminating arsenic and coliform from water using MNB. The chapter is divided into two parts, the first part explains the study conducted on arsenic removal from water while the second part discusses about coliform removal. As discussed in chapter 2, it is evident that arsenic and coliform can be eliminated via oxidation using ozone. Hence O₃ MNBs of different sizes were tested for their oxidation efficiency on arsenic and coliform present at different concentrations. Further method to develop adsorbent and the measurement techniques adopted to quantify arsenic and coliform are also discussed. The objective of the investigations described in this chapter was to study the parameter at which MNB (size range) can provide better oxidation rate for arsenic and coliform. These findings will assist in developing efficient prediction algorithm of MNB.

4.1 REMOVAL OF ARSENIC USING O₃ MICRO-NANO BUBBLE

4.1.1 INTRODUCTION

Arsenic is found in water primarily in the As(III) and As(V) oxidation states. It can be determined both in inorganic and organic forms, while the latter are quantitatively insignificant and is found mostly in areas severely affected by industrial pollution. Inorganic arsenic species are the dominant forms which is usually detected in groundwater, these are more toxic in nature than the organic arsenic. Most of the arsenic removal technologies are effective in removing As(V), As(III) is predominantly non-charged below pH 9.2, therefore most of the sorption techniques can hardly remove As(III). Thus As(V) is much less mobile than arsenite, as it tends to co-precipitate out with metallic cations or to adsorb onto solid surfaces. In this regard, the contaminated water where As(III) is the dominant species needs to be pre-treated by oxidation. Atmospheric

oxygen is the most readily available oxidizing agent and many treatment processes prefer oxidation by air. However, air oxidation of arsenic is a very slow process and can take weeks for oxidation. The effect of bubble size over oxidation process can be observed in figure 4.1. It can be observed that the larger the bubble size, the faster they tend to rise to the surface while the smaller bubbles stay longer in the water which helps in effective oxidation rate.

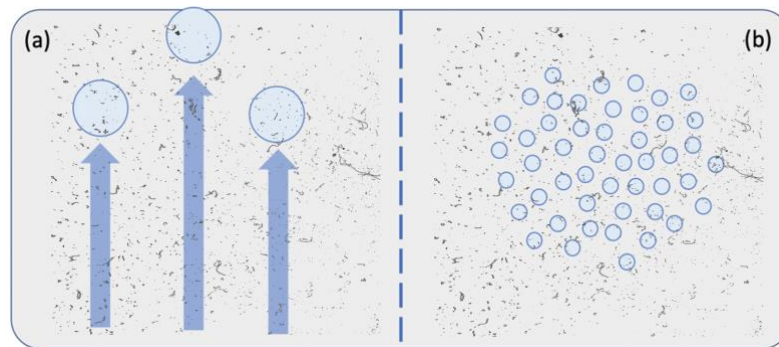


Figure 4.1 Role of bubble size in oxidation rate (a) larger bubble size tend to rise to the surface; (b) smaller bubbles remains in water for longer duration

While ozonation is considered as an alternative option, since ozone is extremely influential oxidant. Therefore, in this study experimentations were performed to understand the efficiency of micro-nano bubble towards ozonation of arsenic for effective removal from water when passed through an adsorbent. The methodology adopted in this study is described in figure 4.2.

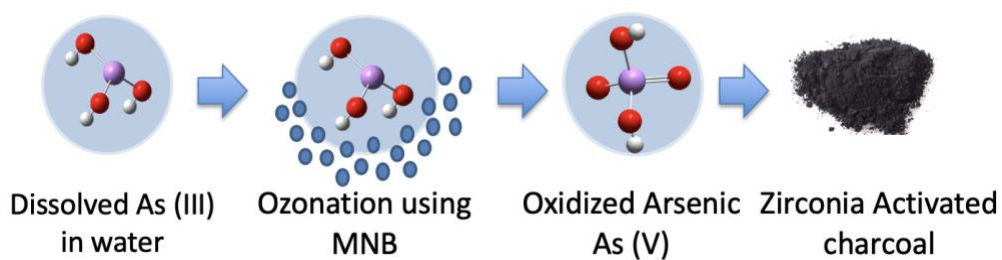


Figure 4.2 Methodology to treat arsenic

4.1.2 MATERIAL AND METHODS

Different concentrations of arsenic spiked water was prepared in 10 L of distilled water while ph of water was maintained at 7. To prepare the aqueous solutions, As standard solution was used to prepare 100ppb, 500ppb, 1000ppb and 4000ppb solutions. MNBs of sizes ranging from 400-500, 700-800 and 1000-1100 nm were generated using ozone gas at a flow rate of 30ml/min. To adsorb As (V), activated carbon powder (150 μ m) from sigma aldrich and zirconium nitrate from sigma aldrich were used to prepare the adsorbent.

4.1.3 SYNTHESIS OF ADSORBENT

The preparation of adsorbent was followed by a method given by okumura et al [126]. In their study, 5.9% of zirconyl nitrate solution was mechanically mixed with 50g of purified activated carbon for 3d at 398 K. Similarly, in this study two different ZrAC adsorbents were prepared having zirconyl nitrate concentration of (a) 5.9 % and (b) 10 % respectively. Synthesis of the adsorbent contained 3 different steps. In the first step, activated carbon with a mesh size of 150 was washed with deionized water several times and dried in oven at 398 K for 24 hrs. In second step, 5.9% and 10% of zirconyl nitrate solutions were prepared by mixing 58.6 g and 110 g of zirconyl nitrate dihydrate in water. In third step, two separate batches of the purified activated carbon (50g) was mechanically mixed with the solutions of zirconyl nitrate solution separately for 3 days at 398 K. The prepared adsorbents were characterized using Scanning Electron Microscope (SEM) to image their surface shown in figure 4.3.

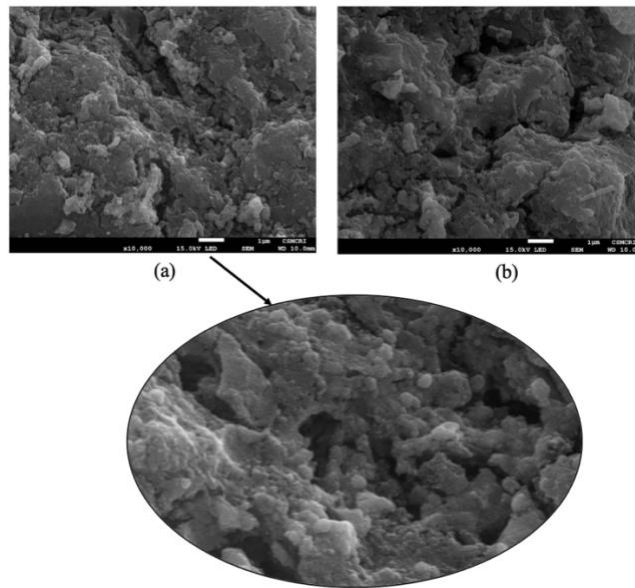


Figure 4.3 Scanning Electron Microscopy (SEM) analysis of ZrAC adsorbents containing (a) 5.9% zirconyl nitrate solution and (b) 10 % zirconyl nitrate solution

It is observed that adsorbent with 5.9% zirconyl nitrate solution showed a rough with layered surface and fine granules. The physical characteristics of figure a, showed more pores and well dispersion of zirconyl nitrate particles over activated carbon. These granules were more visible with diameter ranging to 100nm and were partly aggregated. Therefore, ZrAC adsorbent (5.9%) was used to test for its adsorption capability.

In order to enhance the contact time of As exposure with the adsorbent, a plain sintered glass column (Borosil, bore size:22mm dia, L:500mm, flow rate:1ml/min) was used as shown in figure 4.4. Further, to prevent the loss of adsorbent or washout during filtration process, a fine amount of cotton was used prior adding the adsorbent (10g) into the column. A 50ml of deionized water was poured into the tube which helped the adsorbent to settle down and also allowed to set the flow rate of the liquid passing out.

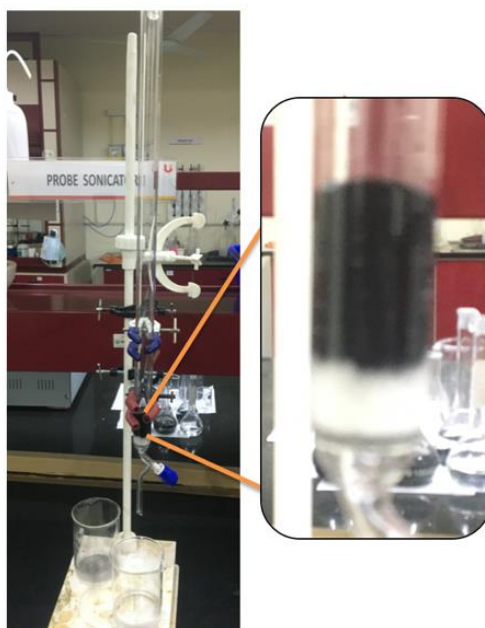


Figure 4.4 Experimental setup of adsorbent in a glass column

In a similar study [106], reports that after zirconium impregnation, the pores are filled with zirconium nanoparticles making the adsorbent more efficient in water treatment process and further it can be repeatedly used without losing the nanoparticles from the pores of activated carbon.

4.1.4 MEASUREMENT OF AS USING ICP-OES

To determine the removal of arsenic, inductively coupled plasma optical emission spectrophotometry ((ICP-OES), PQ 900, Analytik Jena) was used. ICP-OES, is an elemental analysis technique that uses emission spectra of a sample to identify their characteristic emission spectra and quantify by the intensity. Plasma energy is generated via argon gas is supplied to torch coil and a high radio frequency is applied to the coil at the tip thereby ionizing argon to generate plasma. The plasma generated is high in electron density with temperature reaching up to 10000 K, through this energy elements/atoms of a sample are excited. The excited atoms after reaching low energy position release

emission rays which corresponds to the photon a wavelength. Based on the wavelength, the element is quantified w.r.t the intensity of the rays.

4.1.5 RESULTS AND DISCUSSIONS

The treatment procedure included ozonation of water via MNBs for a duration of 30 mins. During treatment process, MNB size was monitored for every 10 mins. After ozonation process, 150 ml of the ozonated water was passed through the adsorbent present in 3 different columns and a sample was collected after filtration to determine the presence of As. The ICP-OES was calibrated at a 11 point scale ranging from 1ppb to 5ppm. As per the software integration process, a correlation coefficient (R^2) value of 0.9950 was attained as shown in figure 4.5.

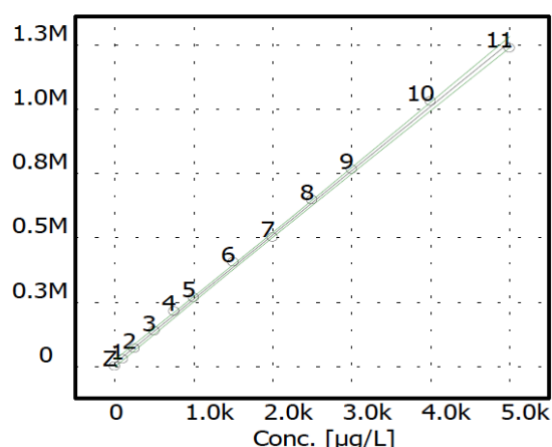
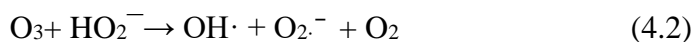
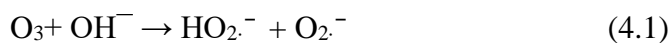
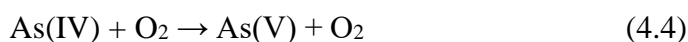
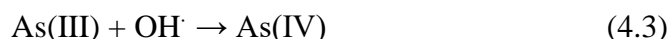


Figure 4.5 ICP-OES instrument calibration graph using As (V) standard at 11 point concentrations

In order to observe the oxidation efficiency of ozone MNB, experiments were conducted at 4 different concentration of As. A study by shows that As(III) ions were able to oxidize by both $\text{OH}\cdot$ and Fe(IV) at a circumneutral pH [127]. During ozonation process a part of the ozone normally decomposes to OH radicals. The elementary reaction mechanism of decomposition of ozone in aqueous solution is as follows.



The radicals that are produced during reaction can introduce other reactions with ozone, causing more formation of $\text{OH}\cdot$. The reaction mechanism for the oxidation of As(III) by $\text{OH}\cdot$ described by Hoigne et al[128].



From figure 4.6 it can be observed that for a fixed concentration of As at 4000 ppb, the conversion of As (III) to As (V) can be seen w.r.t. different size of MNBs.

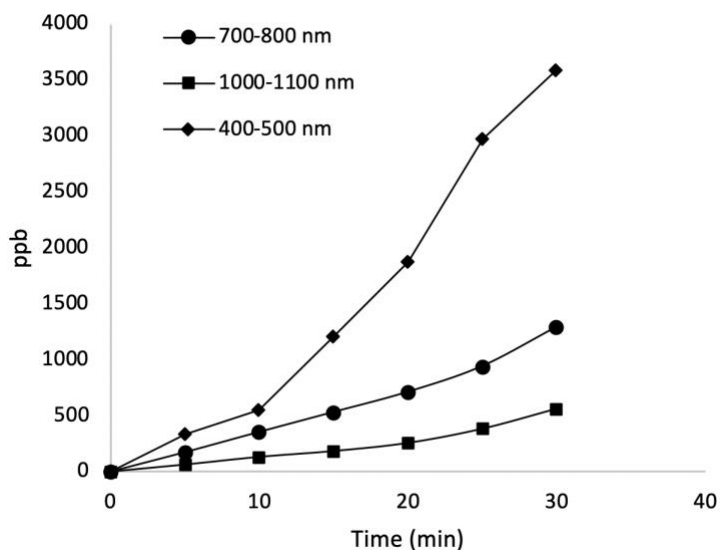


Figure 4.6 Oxidation of As(III) to As(V) using different O_3 MNBs

The initial oxidation seen to be constant for all the MNBs till 5 mins, but as the time duration increased the oxidation varied and the smaller sized MNBs showed better results, this can be due to presence of high internal pressure and large specific area of MNBs. MNBs can persist in water and can reach high

concentration levels, which greatly increase the peak value of the dissolved ozone concentration. Similar results were reported by Li et al.[129], who showed that MNBs significantly increased their mass transfer efficiency of oxygen. The total arsenic concentration was monitored and resulted to be present constant throughout the experiment, indicating the balance of As (III) and As(V) concentrations.

In a study [130] it was observed that at an increased temperature oxidation of As (III) using ozone was not so effective. Batagoda et al. [131] observed that ozone concentration in water reduced rapidly when ozone was sent through a diffuser stone compared to an ultrasonic nano bubble generator. This showed that nanobubbles increased the solubility of ozone in water. It was spotted that As contaminated water oxidized using O₃ MNBs when passed through the adsorbent showed better removal efficiencies with MNBs of 400-500nm when compared with MNBs of 1000-1100nm as shown in figure 4.7. This stays in line with other concentrations of As.

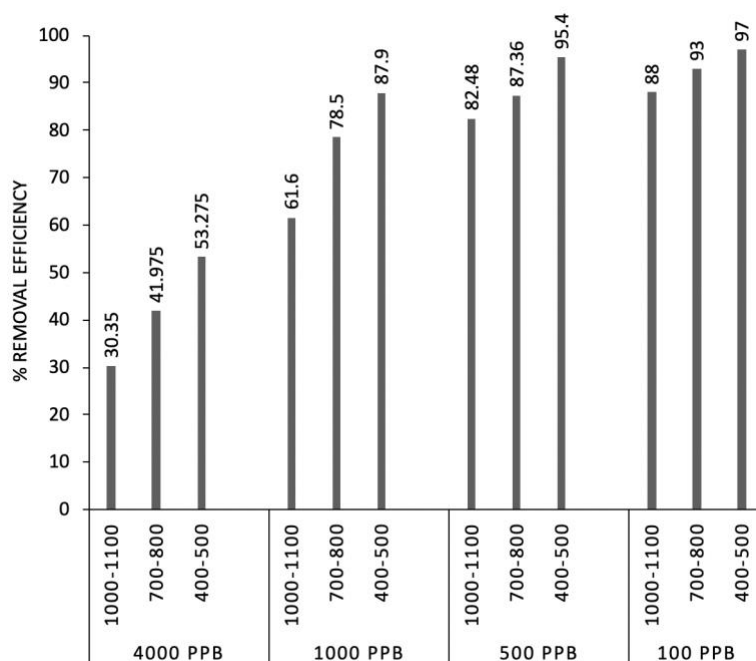


Figure 4.7 O₃ MNBs performance when As contaminated water is treated and passed through the adsorbent

To support the findings of figure 4.7, a qualitative analysis of surface topography was performed using scanning electron microscope (SEM). Energy dispersive X-ray microanalyzer (EDX) (Oxford instruments, England, model:7353) connect with SEM was used to provide elemental identification and quantitative composition of the compound. A sample of adsorbent collected before and after passing the As contaminated water was used for the analysis shown in figure 4.8.

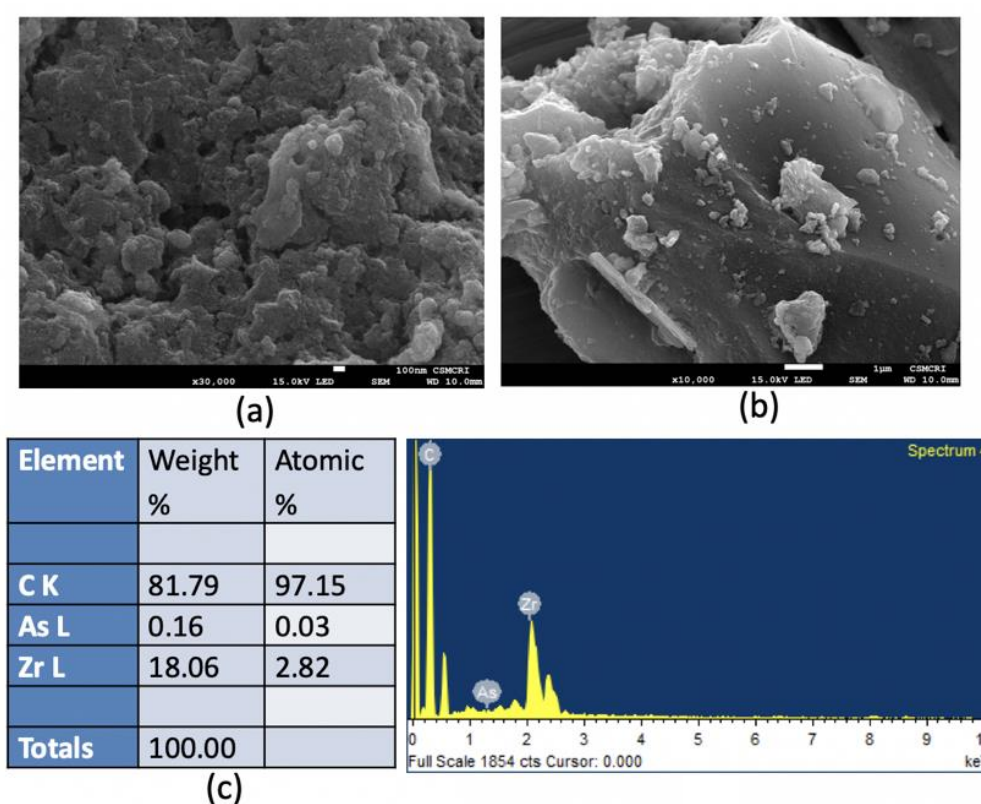


Figure 4.8 SEM-EDX analysis of adsorbent; (a) before adsorption of As(V); (b) after adsorption of As(V); (c) EDX of adsorbent showing presence of As

Figure 4.9. shows the XRD analysis of the adsorbent conducted for structural study shows that adsorption of As (V) have changed the morphology of the adsorbent. The initial peak observed at 2θ 27° was of XRD holder. Presence of arsenic adsorbed on Zr-AC adsorbent can be seen at 2θ 44° showing the adsorption capability.

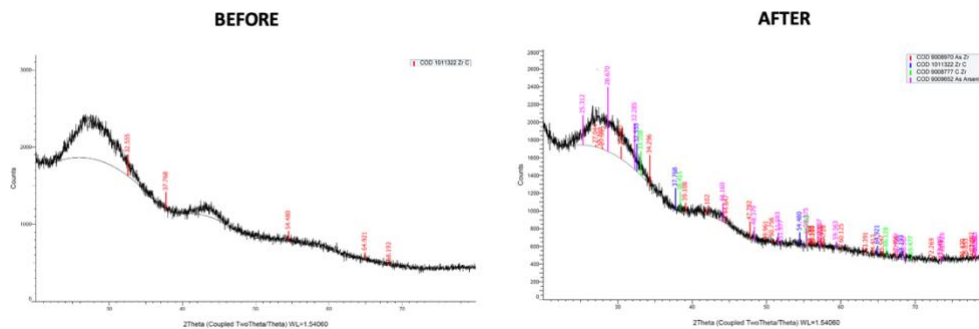


Figure 4.9 XRD analysis of adsorbent before and after adsorption

4.2 REMOVAL OF COLIFORM USING O₃ MICRO-NANO BUBBLE

4.2.1 INTRODUCTION

The coliform group, as stated earlier, includes species of Citrobacter, Enterobacter, Escherichia, Hafnia, Klebsiella, Serratia and Yersinia [132]. Total coliform and fecal coliform organisms are often used in conjunction with specified requirements for treating wastewater. These bacteria can also be found naturally in soil and on vegetation regions. In water, dissolved ozone and free radicals created in ozone-hydroxide reaction makes the oxidation-reduce potential (ORP) of water to increase, since all these are the strong oxidizing agents. Microbes as viruses, bacteria, fungi, moulds can be removed in water with high positive ORP; E. coli is fully killed in water having ORP of 600 mV and higher [133]. The methodology adopted in this study is illustrated in the figure 4.10.

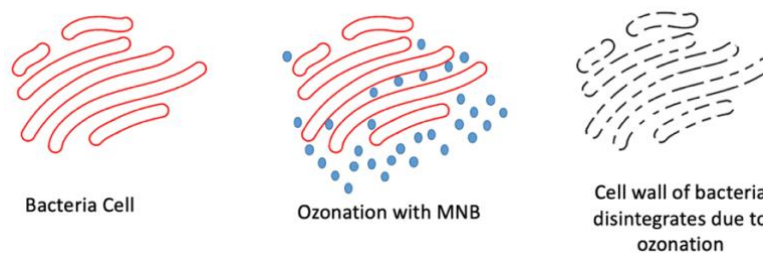


Figure 4.10 Methodology to treat coliform bacteria

4.2.2 MATERIAL AND METHODS

The water containing coliform bacteria from UPES STP (sewage treatment plant) was used for experimentation. Prior experimentation, 2L of STP water was mixed with 8L of tap water. In order to determine the presence of coliform bacteria, agar-based petri plates were used. The process of agar media preparation is illustrated in figure 4.11. After solidification, these petri plates were later stored at 4°C to avoid contamination with a shelf life of not more than 30 days.

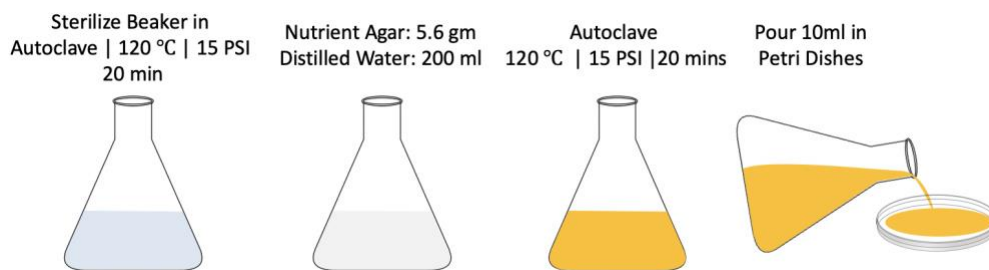


Figure 4.11 Preparation method of nutrient agar media

Since the source of water is from a sewage treatment plant (STP), it is a known that water from a STP will contain colonies in larger amount. Hence serial dilution method was followed for determination of colonies. Figure 4.12 describes the process of serial dilution using saline water.

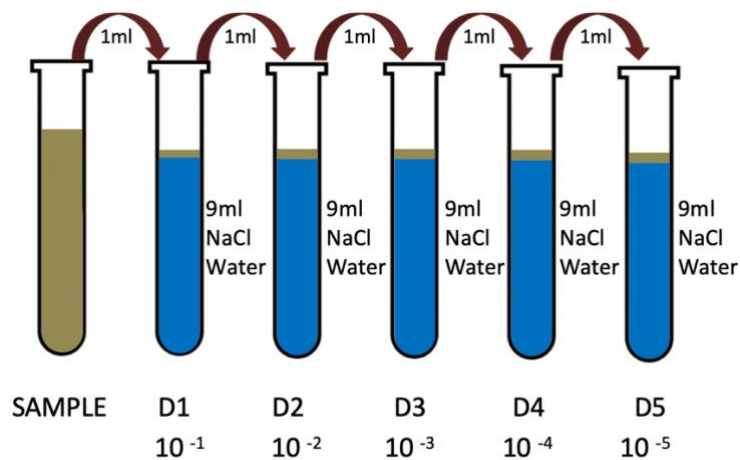


Figure 4.12 Serial dilution procedure of the sample

4.2.3 MEASUREMENT OF COLIFORMS

Ultra HD automatic colony counter (SCAN 4000, Interscience) was used to identify the presence of coliform bacteria. It comes with a 5MP of HD camera, providing live image display on a computer screen. When used in automatic mode, it can count upto 1000 CFU/sec in all different types of media. The identified colonies are marked with a cross mark and the results are saved automatically.

The instrument can be used at 7 different combinations of lighting and enhances the image zoom by X69. This instrument also has a 360° shadow free lighting technology resulting in identification of a 0.05mm sized colony sized.

4.2.4 RESULTS AND DISCUSSION

The experiments were conducted with O₃ MNBs of different sizes ranging from 400-500nm; 700-800nm and 1000-1100 nm. The treatment cycle was kept constant for a duration of 30 min. A 100ml water sample was collected before and after treatment procedure. Every sample was diluted following serial dilution method using NaCl. These diluted samples were later plated in a nutrient agar media in a petri dish prior incubating them at 35°C for 24hrs. The nutrient agar media contained a composition of 15g/l agar, 1g/l meat extract, 5g/l peptone, 5g/l sodium chloride and 2g/l yeast extract. The colonies formed after 24hrs incubation are shown in figure 4.13, determined using SCAN 4000 instrument. E. coli upon incubation tend to appear circular, large, greyish white, smooth and moist like structure.

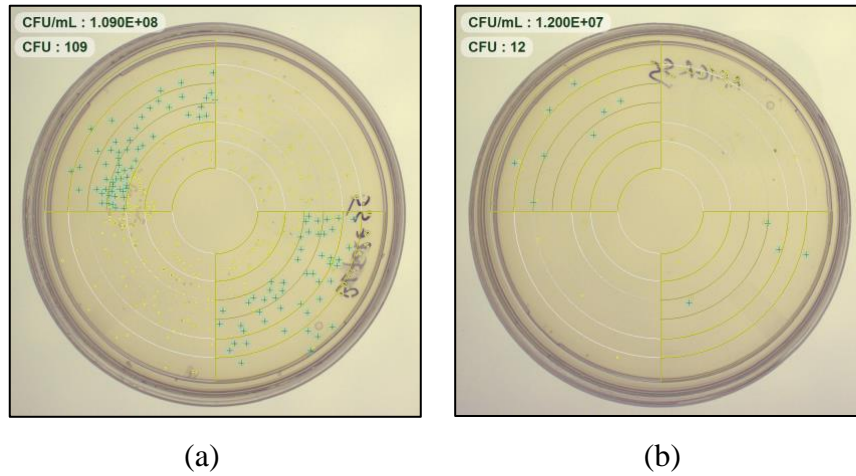


Figure 4.13 Culture of *E.coli* in nutrient agar media; (a) before treatment with O_3 MNB; (b) after treatment with O_3 MNB

Figure 4.14 shows the inactivation of the coliform group w.r.t to MNBs of different size ranges. These results indicated that the mass transfer of ozone is primarily enhanced by increasing both the interfacial area to volume and bubble residence time in the system, however with further decrease in MNB size, the disinfection efficiency is not enhanced.

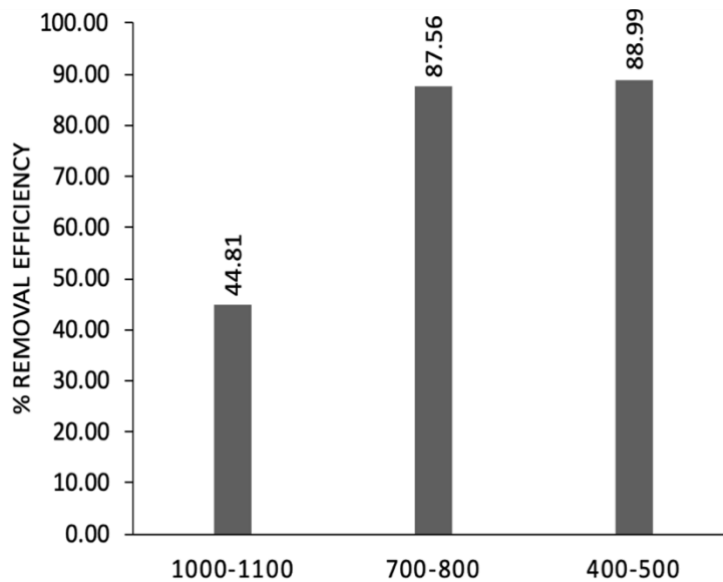


Figure 4.14 Removal efficiency of coliform bacteria using O_3 MNBs

It was observed that exposure of coliform bacteria to ozone MNBs were similar at 700-800nm and 400-500nm range. These bubbles exhibit the possibility that OH radicals and shock waves generated by the collapse of micro-bubbles may have influenced the inactivation of the coliform group effectively. This process of neutralizing or killing a microorganism adopted by ozone is known as cellular lysis. During oxidation process, ozone ruptures the cellular membrane of microorganisms and disperses the bacterial cytoplasm into the solution, thus making reactivation impossible. This process takes place with a relatively low ozone dose for fecal coliform inactivation, because of the fast kinetics between ozone and coliform bacteria. A low ozone dose of 2.4 mg/L using DOF technique have been highly effective in removal of coliform. In the case of UV light usage a proper design of the UV dose with proper balancing of efficiency dose along with energy consumption is necessary for any wastewater treatment plant[134]. In such case, findings showed no difference between LP and MP UV lamps towards photoreactivation of bacteria when evaluated with a HP UV lamp for treatment of coliform in a wastewater treatment plant. The results suggest that use of micro-bubbles in treatment process for ozonation can help in reducing reactor size and ozone dosage.

4.3 SUMMARY

The results indicated the potential of using MNB for effective oxidation and disinfection of arsenic and coliform bacteria respectively. However, in the case of coliform bacteria, the need of smaller size bubbles especially below 500nm was not necessarily required as MNBs of 700-800nm were able to reach similar disinfection efficiency. This contradicted with the results of arsenic oxidation from As(III) to As(V) where smaller MNBs were showing promising results towards effective oxidation. Overall, the results implied that MNBs are capable to be used for oxidation applications.

CHAPTER 5

MICRO-NANO BUBBLE SIZE PREDICTION

This chapter presents a model to predict MNB size. Based on the experimental results obtained in the study carried out during generating different MNBs, the relation between pressure, temperature with bubble size are discussed. Two different machine learning approaches were used to test for its feasibility to avoid sensory dependencies during operation.

5.1 OVERVIEW

To attain better performance of MNB, it is important to maintain the required MNB size during operation. System characteristics such as pressure, temperature and gas flow rate tend to change with time of operation making the system complex to maintain a constant sized MNB. While operating the system for longer durations it was observed that the size of MNB was varying and this was primarily due to the rise in temperature of the water. The deflection in MNB size was in the range of 200-300nm with every 5°C rise in temperature.

In practice, system operator depends upon sensor and instrumental input to understand the bubble size at any point of system operation. Moreover, presence of debris such as dust particles in water, makes it more difficult for the sensors to identify and differentiate a MNB to a debris/dust particle leading to an improper information relayed to the operator. Most studies stating waste water treatment plant as a complex control system and the lack of sensory advancements to detect MNB in nanoscale in the presence of debris makes it more complicated task to automate the generation of MNB of different sizes in larger applications.

With an increase in technology and computational capacities, machine learning (ML) has gained the attention by different industries for its wider application approaches. Specifically in water treatment, ML is used for prediction of COD,

BOD and other parameters to achieve better performance and improved efficiency of a system. Use of such automated control and information technology enables continuous collection of data containing all the required and necessary process information allowing to predict and optimize the processes during operation.

5.2 MACHINE LEARNING APPROACH

Here in this system, we test the use of two different Machine Learning (ML) approach specifically for MNBs generated via pressurized dissolution method. This helps in reducing the dependency on using particle size analyzer for knowing the bubble size being generated. The primary goal of this research is to provide a data driven approach to model and predict the size of micro-nano bubble. The methodology adopted in this study is illustrated in figure 5.1.

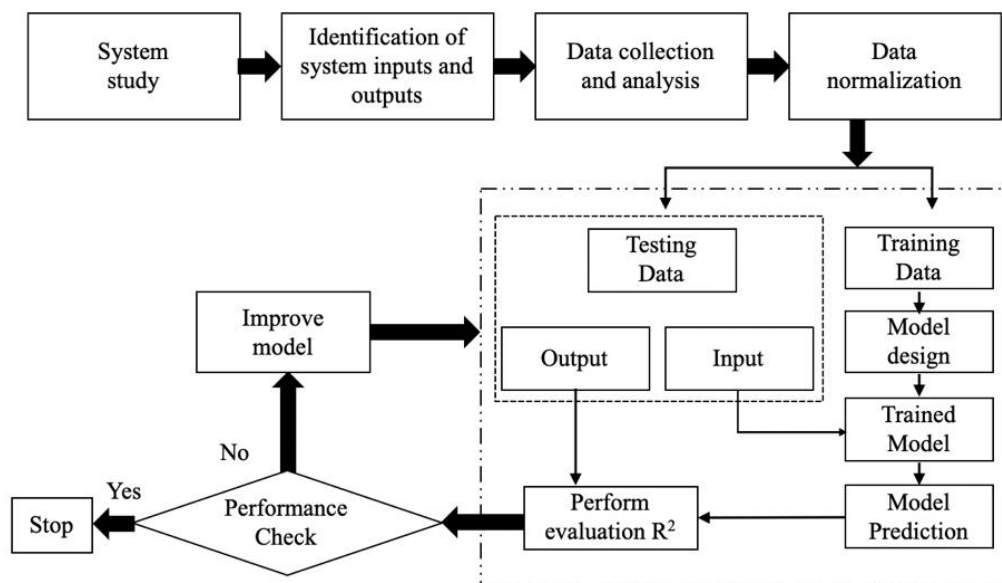


Figure 5.1 Methodology of machine learning models

As discussed earlier most of the applications of MNBs are directly implemented without any addition of surfactants therefore, to test the adaptability of use of ML in predicting MNB size, following assumptions were made

1. No surfactants are used in the system
2. The feed gas flow rate was kept constant at 30 ml/min at 20 PSI
3. Water level present in the system is 20 Ltrs
4. Continuous monitoring of the system parameters is carried out for every 5 minutes during operation

5.2 COMPUTATION OF MNB

Since ML is a data driven approach, the parameters involved in generating MNB of different sizes were recorded in a form as shown in figure 5.2 (a). The data entered in the form was stored in the form of a dataset a sample of which is shown in figure 5.2 (b).

Clear Form		MNB DATABASE FORM		SUBMIT	
Entry ID: 1					
Water Parameters		Surfactants		Bubble Characteristics	
Water Type	NEW	Name	NA	Least Peak (in nm)	220
Water Level in Tank	10	Concentration	0	Z-Average (in nm)	300
<small>vol</small>	<small>12.53</small>	<small>if Multiple use comma</small>		Run	5
FEED GAS		Pump Parameters		Sample Time	1
TYPE	Comp. Air	Input Valve (PSI)	-9	Old Sample Re-run	NO
PSI	20	Output Valve (PSI)	50	Time Difference	0
FLOW	30	Needle Valve	blue	DO Concentration	
PPM Calculator		System Parameters		Before Bubble Gen	
PPM required		System O/P Pressure	80	After Bubble Gen	
Density	1	Pump Run Time	5	Remarks	
Grams	0.0000	Water Temperature	22		
Vol	0.0000				

(a)

Feed Gas	O/P Pressure (psi)	MNB size (nm)	Temp (°C)
Comp Air	80	20	1608
Comp Air	80	20	1635
Comp Air	60	30	3793
Comp Air	60	30	3803
Comp Air	60	35	4735
Comp Air	60	35	4751
Oxygen	60	20	1632
Oxygen	60	25	2556
Oxygen	60	30	3088
Oxygen	80	20	1084
Oxygen	80	20	1144
Oxygen	80	35	2151
Ozone	80	20	390
Ozone	80	20	373
Ozone	80	35	876
Ozone	80	35	879

(b)

Figure 5.2 MNB dataset; (a) data entry form; (b) sample dataset

A three-step modelling approach was incorporated to predict the bubble size. Step 1 included the identification of system operating conditions which has the potential to influence the generation of different MNBs. These parameters included system output pressure, temperature and gas type. Step 2, focuses on the data entries to sort and identify any missing data and if so, these data were addressed by approximating the relationship between the identical parameters. In step 3, modelling approaches are interpreted for their error and efficiency in predicting MNB size.

ML algorithms methods are categorized as (a) regression and (b) classification method. System in which output variables are discrete in nature falls under classification algorithm. However, systems where output variables vary continuously falls under regression algorithm models. Since the output of our system is varied continuously, regression algorithm is considered in this study for MNB size estimation parameters. Regression analysis approach is a process for estimating relationships between the variables effecting system[135]. These systems usually contain single output response based on multi or single input variable. There are different types of regression techniques typically applied depending on type of correlation between the variables. These include linear, polynomial and logistic. In the stated application case though there are number of variables the behaviour of the variables is primarily linear. Of the different ways, for multi variable processing regression approaches typically aim for categorization. Classification methods at times support both continuous and categorical data with limited computational cost. In this particular application though the mechanism is prediction of specifications of parameters leading to generate different MNBs, it can also be visualized as classification of variables (ranges) to their respective type or volume of bubble (class). Hence Classification And Regression Tress (CART) is a effective method for this problem case. Variable tendencies having linear behaviour and

nondeterministic approach decision systems (classifier) are typically used. In the given context the number of variables considered are water temperature, system pressures, gas type, gas flow rate; indicate not only linear relation but also linear correlation. Hence initial and stable classifier (decision tree) with limited number of classes is considered. The advantages of decision tree is stability with high dimensional data and stable accuracy. This inductive approach provided by the decision tree is very effective when no specificities on the domain knowledge is considered. The decision tree-based model has many advantages [136]: a) Ability to handle both data and regular attributes; b) Insensitive to missing values; c) High efficiency, the decision tree only needs to be built once. Decision tree-based models may have faster calculation speed and are more conducive to short-term prediction. Moreover, water quality monitoring data sometimes have missing values due to equipment failure, the decision tree-based model has an advantage in forecasting.

5.2.1 RELATIONSHIP BETWEEN THE PARAMETERS

Parameters are important in ML algorithms. These form a part of the model design using training data to develop prediction. Parameters consist of different variables categorised as dependent and independent variables. These variables can be any number, quantity or any characteristics which can be measured or counted. They are termed as variable due to their value which can be changed or varied over a period of time. Any variable which can be controlled and is not varied due to change of other variables is classified as an independent variable whereas variables which tend to depend on other variable values are termed as dependent variables. In this study of generating MNBs of different sizes using pressurised dissolution method, the size of MNB is our dependent variable whereas the following were identified as an independent variable

1. Output pressure of the system
2. Water temperature
3. Gas

5.3 LEARNING BASED ESTIMATION

Estimation based learning approach is being used more than statistical hypothesis given to its much easier way to analyze, interpret a data in any given research context particularly in machine learning approaches. Several methods and models are being used in ML depending on the complexities and the need of precision in prediction of an algorithm. In this study where the parameters are nonlinear and dependent parameters are very less, the need of higher algorithms can be eliminated and stable statistical approaches can be implemented. In machine learning majority of prediction problems are usually solved with classification and regression methods.

Where, a classification is a process of finding a function or a model which separates a data into several categorical classes. The data is labeled in different classifications according to the parameters given. These models are used where the data is able to be divided into binary or multiple labels. While in regression, a model or a function is used for finding and distinguishing a data into continuous real values. It models a targeted value based on independent variables. Few areas where this model is most widely used are forecasting, finding effective relationship between variables. This model provides an equation which explains a relationship between the parameters. There are different types of regression models of which linear and multilinear regression models are widely used. Linear regression helps to quantify a relationship between one predictor variables and one outcome variable whereas multi linear regression uses multiple variables to predict an outcome of a variable.

5.4 ALGORITHM

The use of regression analysis in this system is described in an algorithm as follows

Step 1: Identifying dependent and independent variables

- Step 2: Explore the dataset and to look out for any missing value, if any value is found they were addressed by approximating the relationship between the identical parameters missing. Cleaning the dataset for any duplicate entries, errors and majorly datatype conversions.
- Step 3: Dataset is distributed into two sets, (a) training set and (b) test set in 3:1 ratio
- Step 4: A relationship between every individual independent variable and dependent variable is drawn using training set
- Step 5: Train the model using different ML approach, this step is to check if the model is able to make predictions correctly
- Step 6: Evaluate the ML model using test set data and check for the prediction probability
- Step 7: Tune the ML model parameters based on the requirements for improved predictions

5.5 REGRESSION MODELS

A. DECISION TREE

Decision tree is a kind of support tool which makes use of a tree like graph model depicting every possible consequences and event outcomes for a prediction model and are capable to handle categorical and numerical datasets. The model breaks the complete data sets into smaller subsets. These subsets are associated with the tree in the form of decision nodes and leaf nodes. A root node forms the topmost node of the tree corresponding to a best predictor. Decision node contains two or more branches representing values for individual attribute tested, decision on a particular numerical target are represented by leaf node. Each node consists of an attribute or feature which is further split into more nodes as we move down the tree.

To determine the decision metric or attribute which is to be used as a root node and other variables to be used as leaf nodes, splitting measures are used such as gini index. These methods help to decide the relevance and importance of every

individual variable. It helps to place the most relevant root node and further as the tree moves down by splitting the nodes the uncertainty decreases leading to a better and effective split at every node.

Gini index measures a degree or probability of a variable which is being wrongly classified when chosen randomly. this degree varies between 0 and 1, 0 implies that all the element corresponds to a certain class and 1 represents that elements are distributed randomly across several classes. Gini Index can be represented using the formula given in equation (5.1).

$$\text{Gini} = 1 - \sum_{i=1}^n (p_i)^2 \quad (5.1)$$

Where p_i is the probability of an object being classified to a particular case. When a decision tree is built, it is preferred to choose the variable having the least Gini index as a root node. The decision tree for predicting MNB size developed is shown in fig.5.3.

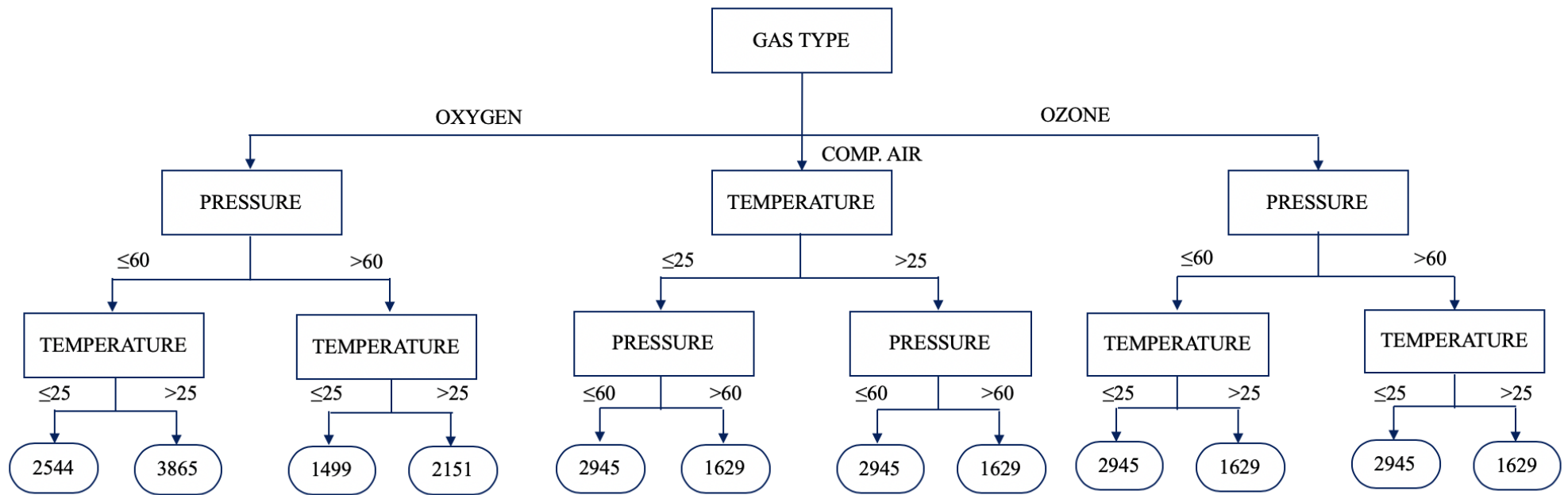


Figure 5.3 Decision tree model to predict MNB size

Here, the test node N has two possible outcomes, corresponding to the conditions $A \leq \text{split point}$ and $A > \text{split point}$. In practice a split point is considered as a midpoint of two known adjacent value of A, in this particular case it is taken as a median. We use Standard Deviation (SD) to calculate the homogeneity of a numerical sample. The stds of different attributes are given in table.

Table 5.1 Standard deviation (SD) of attributes

Attribute	Variables	SD	Count
Gas Type	Comp Air	939.51	160
	Oxygen	865.08	160
	Ozone	578.20	160
Pressure	≤ 60	1041.14	240
	> 60	1049.13	240
Temperature	≤ 25	764.91	240
	> 25	1233.80	240

Based on the attributes SD, the root node is selected, std of both size and gas type can be derived as

$$\sum \text{Probability}(c) * \text{std}(c) \quad (5.2)$$

Where c is category of the attribute

$$\text{i.e., } (1/3 * 939.5128) + (1/3 * 865.08) + (1/3 * 578.20) = 794.266$$

While std of size and pressure is 1045.141 and std of size and temperature is 999.358. Selection of split nodes are calculated based on standard deviation reduction after a data is split on an attribute. Construction of decision tree from here is finding the attribute returning a highest std reduction values i.e., the most homogeneous branch, the std reduction of the attributes is described in table 5.2.

Table 5.2 SD reduction of the attributes

Attribute	SD	SD reduction
Gas Type	794.26	352.83
Pressure	1045.14	101.962
Temperature	999.358	147.745

The std reduction is observed to be highest in the case of gas type, therefore it is considered as a root node. Similarly, as the tree is being built, std and std deviation was calculated for the sub tree until the there are no attributes are present to select or define when the std of the attribute is 0.

While conducting test runs for the evaluation of the decision tree model with the test set data, it was observed that the decision tree model was giving an error of ± 1200 nm in size and therefore to further clear and analyze the data linear regression model with multiple parameters were considered.

B. MULTI LINEAR REGRESSION MODEL

Multiple linear regression explains the relationship between one continuous dependent variable (y) and one or more independent variable (x). It is a continuous dependent variable since y is the sum of the independent variables. Therefore relations ship between parameters were drawn using training set database. Since the final aim was to predict MNB size, relationship between different parameters were drawn for individual feed gases.

For Compressed air, MNB size can be predicted using

$$\text{Size}=48.166\text{Temp}-49.568\text{Pressure}+5366.194 \quad (5.3)$$

An error of ± 121 nm, was observed when the model was tested with the test set.

Similarly, for Oxygen, MNB size can be predicted using

$$\text{Size}=30.680\text{Temp}-6.004\text{Pressure}+159.128 \quad (5.4)$$

When this was tested with test set data, and error of ± 87 nm was observed.

For Ozone, the MNB size can be predicted using equation (5.5), which resulted in an error of ± 94 nm

$$\text{Size}=54.105\text{Temp}-67.099\text{Pressure}+5530.59 \quad (5.5)$$

5.5. EVALUATION

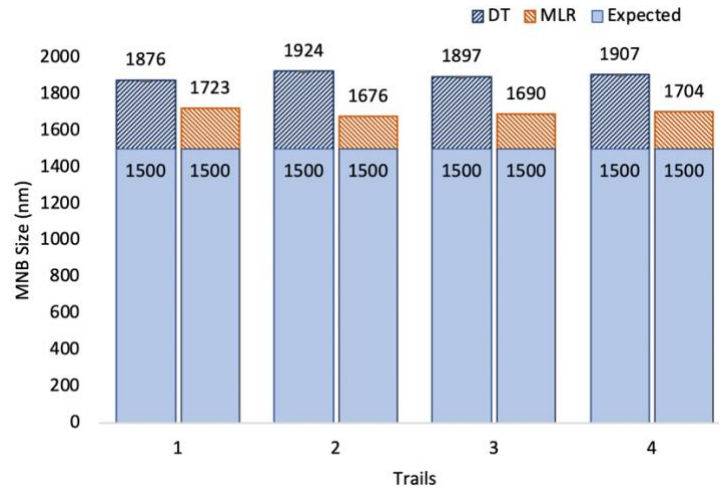
To evaluate the prediction models efficiency in real time scenario, variables such as temperature and pressure were predicted using decision tree and multi linear regression model for different MNB sizes. Based on the experimental results obtained in chapter 3, the upper limit and lower limits of MNB size generation possibilities were determined as given in table 5.1 in absence of any surfactants. Hence the experimental validations were carried out in the respective size range for a duration of 5 mins prior estimating the MNB size generated.

Table 5.3 Minimum and maximum prediction ranges of MNB ML models

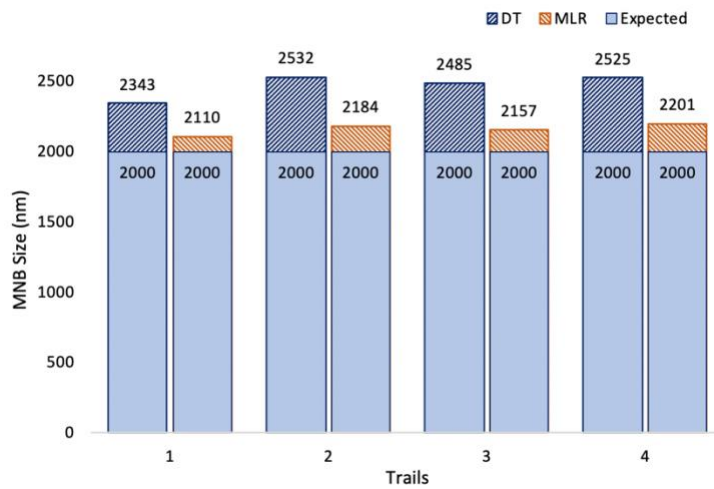
Feed Gas	Minimum (in nm)	Maximum (in nm)
Compressed Air	2000	4000
Oxygen	1000	2000
Ozone	300	1000

Figure 5.4 – 5.6 illustrates MNB size generated using decision tree and multi linear regression models. An estimated value was selected and used in the model to provide the necessary parameters values of pressure and water temperature.

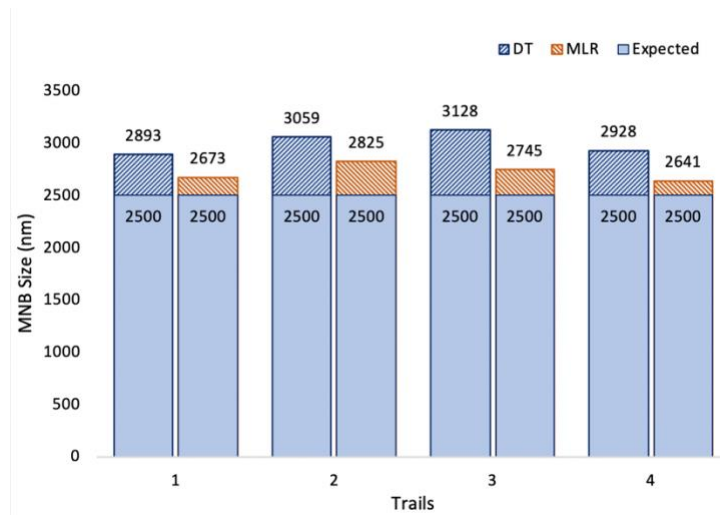
These parameters were then entered into the system and monitored during experimentation trails. Four individual runs were performed for every estimated value and the error was monitored to understand the better performing model.



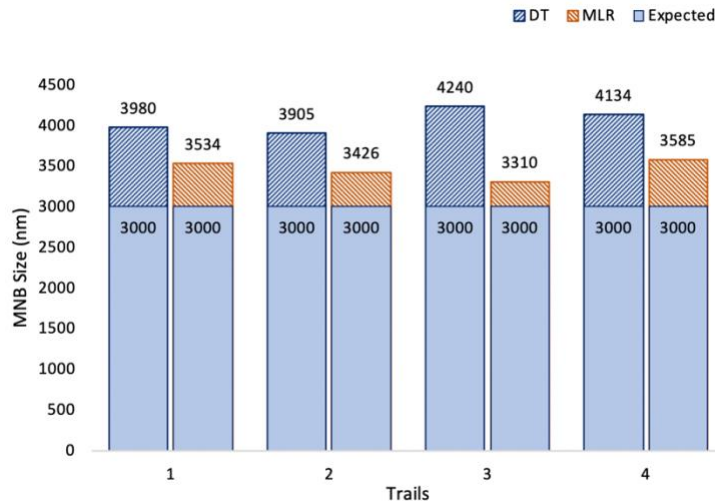
(a)



(b)



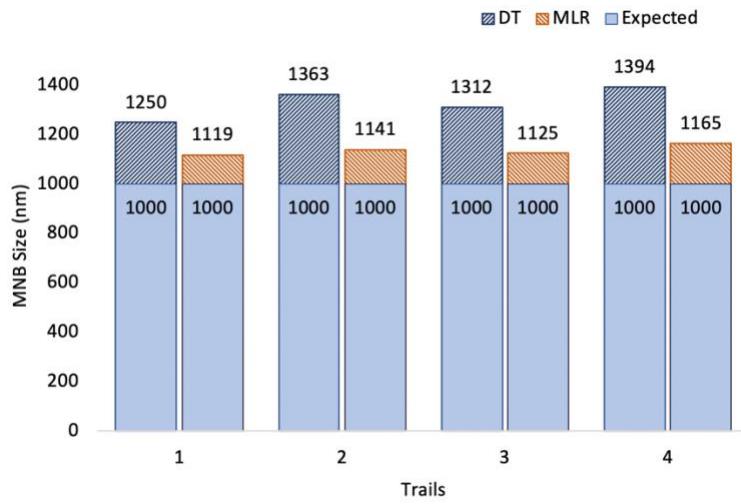
(c)



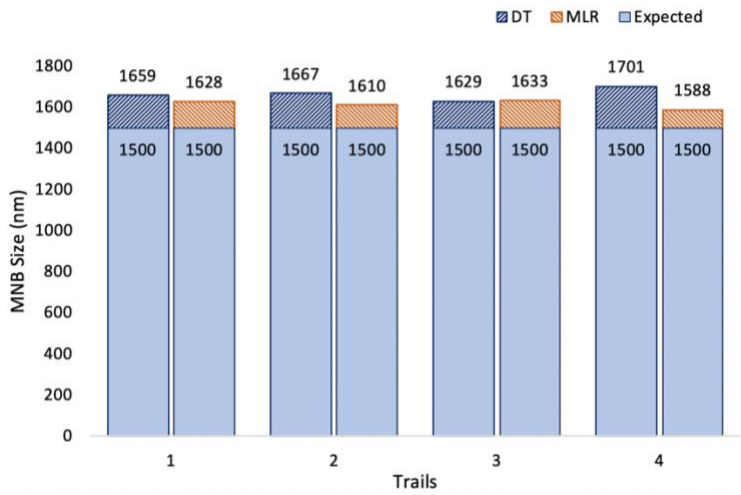
(d)

Figure 5.4 Prediction models evaluation for compressed air MNBs of (a) 1500nm; (b) 2000nm; (c) 2500nm; (d)3000nm

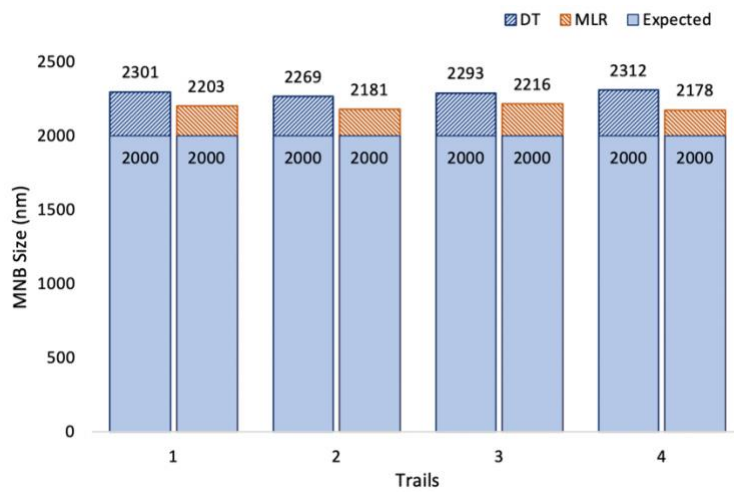
Based on the above fig 5.4. it is observed that the performance of multi linear regression is better against decision tree. However, when it comes to the amount of error percentage recorded, decision tree has shown an incremental behavior ranging from 20-35% while multi linear regression reflected inverted gaussian behavior ranging from 8-15%. It appears when the compressed air is the medium, multi linear regression methodology can optimally MNB of 2000-3000nm with 8% error.



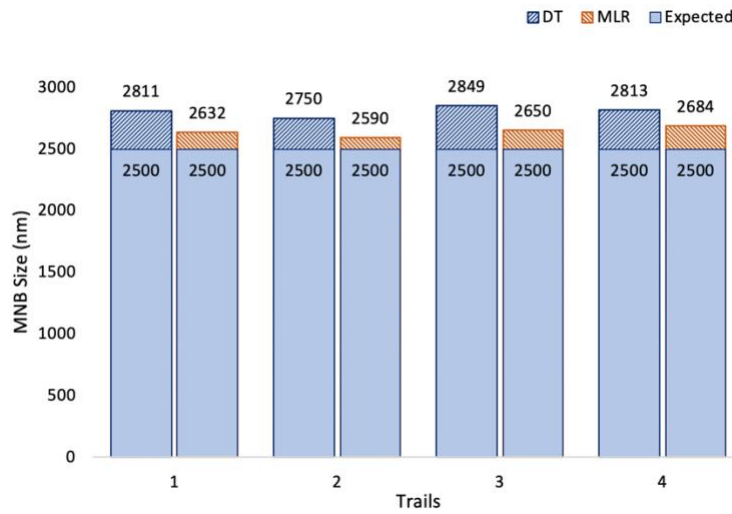
(a)



(b)



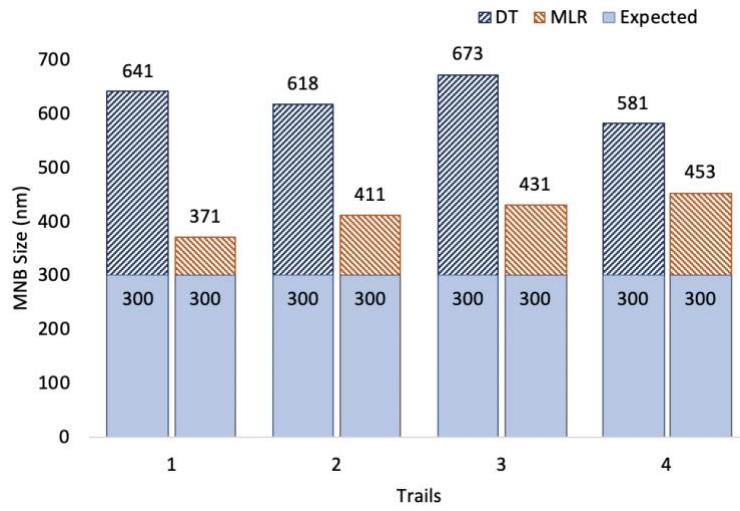
(c)



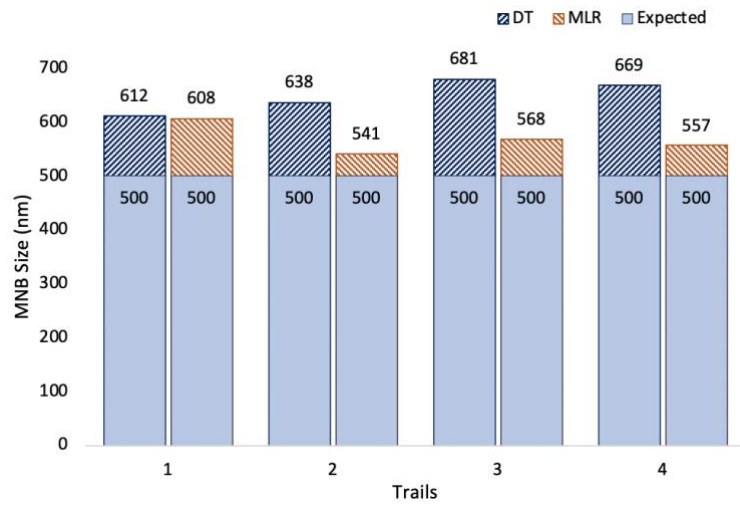
(d)

Figure 5.5 Prediction models evaluation for O_2 MNBs of (a) 1000nm; (b)1500nm; (c)2000nm; (d) 2500nm

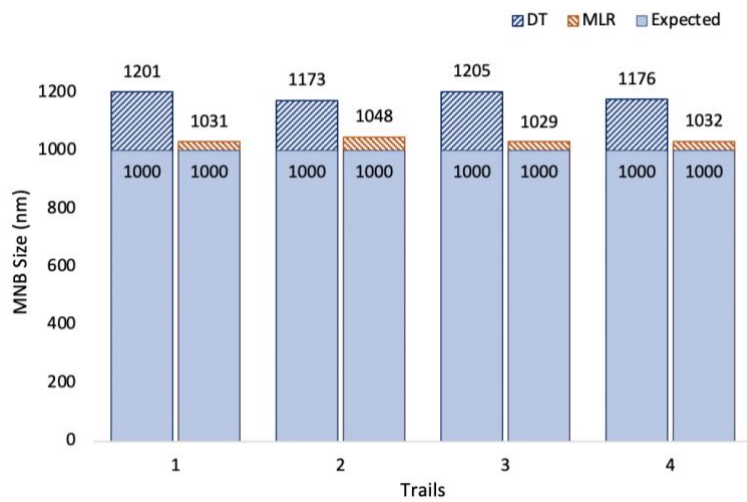
In the case of oxygen gas, both decision tree and multi linear model showed a decremental behavior in error percentages as the size of MNB was increased. An error of 15-35% was observed in fig.5.5 for decision tree model and around 6-13% error was seen for multi linear regression mode. It appears that in higher MNB sizes the models were able to provide better estimation with an error of 12% in decision tree and 6% in multi linear model capable to generate 2500nm of MNB.



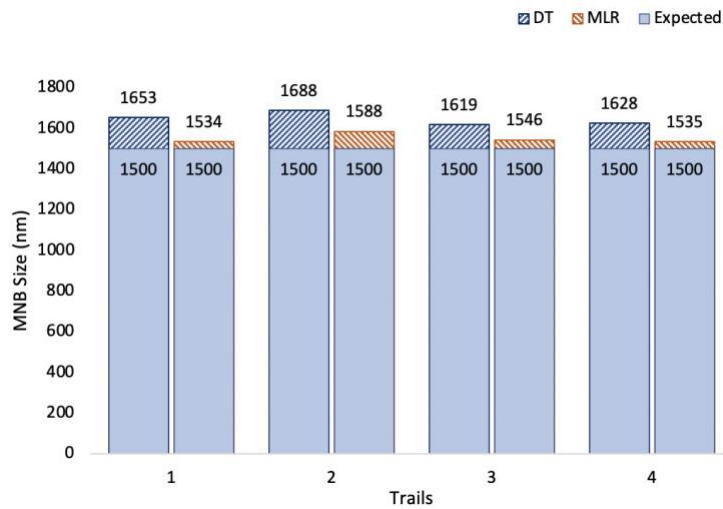
(a)



(b)



(c)



(d)

Figure 5.6 Prediction model evaluation for O_3 MNBs of (a) 300nm; (b) 500nm; (c) 1000nm; (d) 1500nm

From figure 5.6, it can be seen that both decision tree models and multi linear regression models resulted and error percentage of 10-30% and 4-13% of error respectively. However, decision tree model failed to predict the smaller range of ozone MNB while multi liner model could predict with 40% of error. Overall in comparison with oxygen MNB prediction model, ozone gas showed a similar like behavior.

The predicted MNB size are generally in agreement with the experimental data. However, results showed that overall multi linear regression model was showing minimal error to predict MNB size prediction than decision tree. This could be due to the linear relation between MNB size with pressure and MNB size with water temperature. It can be seen that the error percentage of the MNB size generated than the estimated bubble size was in the range of 15-23% in the case of decision tree and 5-14% for multi linear regression model. It was found that prediction of MNB size using pressure, water temperature and feed gas is feasible, however in order to increase the efficiency, other parameters such as gas flow rate, surfactants concentrations can be also used.

5.6 SUMMARY

The chapter presents the applicability of different machine learning algorithms in predicting MNB size. The prediction of bubble size is based on system operating pressure, water temperature and feed gas. In a whole, a decision tree model was developed which showed higher error values where multi linear regression model was used to reduce the error gap. The results achieved were promising and its expected that by incorporating prediction models, the need of sophisticated instrumentation to analyse MNB size during operation can be neglected. It is suggested that the incorporation of other variables such as gas flow rate, surfactants can further reduce the error and improvise the prediction model efficiencies.

CHAPTER 6

CONCLUSION AND FUTURE WORK

The chapter draws conclusion and summarises the entire work presented in the thesis. The details of thesis contributions and the future works of the research are discussed.

6.1 CONCLUSION

MNB has wide potential applications for implementation. Different applications may require a different size, maintaining and monitoring a particular size for longer duration remains a challenge. Under various operational conditions, the size of MNB changes. Due to its size ranging in nm to μm , gives a challenge to the sensors and other instrumentations responsible to identify the bubble size being generated. Presence of debris and other minute dust particles in water makes it more difficult to differentiate a MNB and estimate the size.

The main objective of this work is to demonstrate a proof of concept model, where a machine learning approach is incorporated in predicting a bubble size. While the potential of MNB in treating arsenic and coliform from water is also studied.

The results indicated that, MNBs of 300-400nm showed better oxidation capabilities than the bubbles of 1000-1100 μm . However, it was observed that bubbles of 300-400nm were able to achieve at lower temperature region below 20°C at a high pressure range. Maintaining such pressure resulted an increase of water temperature as a by-product thereby increasing MNB size gradually. this showed an equal importance of temperature, pressure and also the gas feed as individual parameters affecting the size of MNB.

6.2 REMOVAL OF ARSENIC AND COLIFORM FROM WATER

Arsenic present in the water was able to oxidise using O₃ MNBs. The rate of oxidation of As(III) to As(V) was studied for MNB different size ranges which showed better ability of smaller sizes than larger bubbles. The trend remained similar in case of coliform bacteria. However, bubbles ranging below 500nm showed equal coliform disinfection percentages.

6.3 MNB SIZE PREDICTION

Regression based machine learning approaches, decision tree and multi linear regression models were used to test the feasibility in predicting MNB sizes. Based on the experimental datasets, the models were capable to predict the size though resulting in 20-30% of error. Multi linear regression-based model showed better performance with an error ranging from 5-15% in bubble prediction. This shows that machine learning approaches can be used to develop an automated solution towards a fully functional MNB application plant setup.

6.4 SCOPE OF FUTURE WORK

In this work, machine learning was used as an approach towards generating a particular size of MNB using pressurised decompression based MNB generation method. Still, some more works are required for complete practicality use of the system.

- The experimental datasets needs to be increased further in nm to μm range, which will help in further reducing the error percentages.
- Different ML algorithms and models can be used to further fine tuning, clearing the dataset which can help in better estimations.
- Incorporation of surfactant-based studies for ML can help in developing systems where its need is necessary.

REFERENCES

- [1] M. M. Mekonnen and A. Y. Hoekstra, “Sustainability: Four billion people facing severe water scarcity,” *Sci. Adv.*, vol. 2, no. 2, p. e1500323, Feb. 2016, doi: 10.1126/sciadv.1500323.
- [2] U. A. Amarasinghe, T. Shah, and B. K. Anand, “India’s water supply and demand from 2025-2050: business-as-usual scenario and issues,” 2008, doi: 10.22004/AG.ECON.235165.
- [3] D. Dudgeon *et al.*, “Freshwater biodiversity: Importance, threats, status and conservation challenges,” *Biological Reviews of the Cambridge Philosophical Society*, vol. 81, no. 2. Cambridge University Press, pp. 163–182, May 2006, doi: 10.1017/S1464793105006950.
- [4] E. A. Abdel-Aal, M. E. Farid, F. S. M. Hassan, and A. E. Mohamed, “Desalination of Red Sea water using both electrodialysis and reverse osmosis as complementary methods,” *Egypt. J. Pet.*, vol. 24, no. 1, pp. 71–75, Mar. 2015, doi: 10.1016/j.ejpe.2015.02.007.
- [5] D. Parvathi, C., and Yajanthini, “Water Resource in India: Considerable Empirical Evidence,” *Int. J. Manag. Dev. Stud.*, vol. 3, no. 11, pp. 1–12, 2014.
- [6] M. Buragohain, B. Bhuyan, and H. P. Sarma, “Seasonal variations of lead, arsenic, cadmium and aluminium contamination of groundwater in Dhemaji district, Assam, India,” *Environ. Monit. Assess.*, vol. 170, no. 1–4, pp. 345–351, Nov. 2010, doi: 10.1007/s10661-009-1237-6.
- [7] L. R. Varalakshmi and A. N. Ganeshamurthy, “Heavy metal contamination of water bodies, soils and vegetables in peri urban areas of Bangalore city of India,” 2010.
- [8] A. Kumar and S. K. Maiti, “Assessment of potentially toxic heavy metal contamination in agricultural fields, sediment, and water from an abandoned chromite-asbestos mine waste of Roro hill, Chaibasa, India,” *Environ. Earth Sci.*, vol. 74, no. 3, pp. 2617–2633, Aug. 2015, doi: 10.1007/s12665-015-4282-1.

- [9] B. P. Naveen, J. Sumalatha, and R. K. Malik, “A study on contamination of ground and surface water bodies by leachate leakage from a landfill in Bangalore, India,” *Int. J. Geo-Engineering*, vol. 9, no. 1, pp. 1–20, Dec. 2018, doi: 10.1186/s40703-018-0095-x.
- [10] R. Reza and G. Singh, “Heavy metal contamination and its indexing approach for river water,” *Int. J. Environ. Sci. Technol.*, vol. 7, no. 4, pp. 785–792, Sep. 2010, doi: 10.1007/BF03326187.
- [11] R. Khan, S. H. Israili, H. Ahmad, and A. Mohan, “Heavy metal pollution assessment in surface water bodies and its suitability for irrigation around the Neyevli lignite mines and associated industrial complex, Tamil Nadu, India,” in *Mine Water and the Environment*, Sep. 2005, vol. 24, no. 3, pp. 155–161, doi: 10.1007/s10230-005-0087-x.
- [12] K. Balakrishna, A. Rath, Y. Praveenkumarreddy, K. S. Guruge, and B. Subedi, “A review of the occurrence of pharmaceuticals and personal care products in Indian water bodies,” *Ecotoxicology and Environmental Safety*, vol. 137. Academic Press, pp. 113–120, Mar. 01, 2017, doi: 10.1016/j.ecoenv.2016.11.014.
- [13] A. K. Krishna and P. K. Govil, “Heavy metal contamination of soil around Pali Industrial Area, Rajasthan, India,” *Environ. Geol.*, vol. 47, no. 1, pp. 38–44, Dec. 2004, doi: 10.1007/s00254-004-1124-y.
- [14] M. Dinesh Kumar Tushaar Shah, “IWMI·TATA Groundwater Pollution and Contamination in India: The Emerging Challenge.”
- [15] A. Agrawal, R. S. Pandey, and B. Sharma, “Water Pollution with Special Reference to Pesticide Contamination in India,” *J. Water Resour. Prot.*, vol. 02, no. 05, pp. 432–448, May 2010, doi: 10.4236/jwarp.2010.25050.
- [16] D. Chakrabarti, H. Rashid, and M. M. Rahman, “Arsenic: Occurrence in Groundwater ☆,” *Encycl. Environ. Heal. 2nd Edition*, pp. 1–16, 2018, doi: 10.1016/B978-0-12-409548-9.10634-7.
- [17] D. Chakraborti *et al.*, “Groundwater arsenic contamination in the ganga river basin: A future health danger,” *International Journal of Environmental Research and Public Health*, vol. 15, no. 2. MDPI AG,

Feb. 01, 2018, doi: 10.3390/ijerph15020180.

- [18] K. CP, “Status and Mitigation of Arsenic Contamination in Groundwater in India,” *Int. J. Earth Environ. Sci.*, vol. 1, no. 1, 2015.
- [19] D. Sukumaran, D. Barui, and R. Saha, “Water Health Status in Lower Reaches of River Ganga, India,” *Appl. Ecol. Environ. Sci.*, vol. 2, no. 1, pp. 20–24, 2014, doi: 10.12691/aees-2-1-3.
- [20] M. M. R. and D. C. Amitava Mukherjee, Mrinal Kumar Sengupta, M. Amir Hossain, Sad Ahamed, Bhaskar Das, Bishwajit Nayak, Dilip Lodh, “Arsenic Contamination in Groundwater: A Global Perspective with Emphasis on the Asian Scenario,” *J. Heal. Popul. Nutr.*, vol. 24, no. 2, pp. 142–163, 2006.
- [21] A. Elisha Onyango, M. Wandayi Okoth, C. Nkirote Kunyanga, and B. Ochieng, “Microbiological Quality and Contamination Level of Water Sources in Isiolo County in Kenya,” 2018, doi: 10.1155/2018/2139867.
- [22] N. J. Ashbolt, “Microbial contamination of drinking water and disease outcomes in developing regions,” in *Toxicology*, May 2004, vol. 198, no. 1–3, pp. 229–238, doi: 10.1016/j.tox.2004.01.030.
- [23] J. P. S. Cabral, “Water microbiology. Bacterial pathogens and water,” *International Journal of Environmental Research and Public Health*, vol. 7, no. 10. Multidisciplinary Digital Publishing Institute (MDPI), pp. 3657–3703, Oct. 2010, doi: 10.3390/ijerph7103657.
- [24] U. S. T. Department, “Bacterial standard for drinking water.,” *Public Heal. Rep.*, vol. 29, pp. 2959–2966, 1914.
- [25] D. Baris *et al.*, “Elevated Bladder Cancer in Northern New England: The Role of Drinking Water and Arsenic,” *J. Natl. Cancer Inst.*, vol. 108, no. 9, 2016, doi: 10.1093/jnci/djw099.
- [26] Y. Zhang *et al.*, “Human health risk assessment of groundwater arsenic contamination in Jinghui irrigation district, China,” *J. Environ. Manage.*, vol. 237, pp. 163–169, May 2019, doi: 10.1016/j.jenvman.2019.02.067.
- [27] S. Wang and C. N. Mulligan, “Occurrence of arsenic contamination in Canada: Sources, behavior and distribution,” *Sci. Total Environ.*, vol.

- 366, no. 2–3, pp. 701–721, Aug. 2006, doi: 10.1016/j.scitotenv.2005.09.005.
- [28] P. Wongsasuluk, S. Chotpantarat, W. Siriwong, and M. Robson, “Heavy metal contamination and human health risk assessment in drinking water from shallow groundwater wells in an agricultural area in Ubon Ratchathani province, Thailand,” *Environ. Geochem. Health*, vol. 36, no. 1, pp. 169–182, Feb. 2014, doi: 10.1007/s10653-013-9537-8.
- [29] Y. Gan, Y. Wang, Y. Duan, Y. Deng, X. Guo, and X. Ding, “Hydrogeochemistry and arsenic contamination of groundwater in the Jiangnan Plain, central China,” *J. Geochemical Explor.*, vol. 138, pp. 81–93, Mar. 2014, doi: 10.1016/j.gexplo.2013.12.013.
- [30] L. M. Camacho, M. Gutiérrez, M. T. Alarcón-Herrera, M. de L. Villalba, and S. Deng, “Occurrence and treatment of arsenic in groundwater and soil in northern Mexico and southwestern USA,” *Chemosphere*, vol. 83, no. 3. Pergamon, pp. 211–225, Apr. 01, 2011, doi: 10.1016/j.chemosphere.2010.12.067.
- [31] D. Chakraborti *et al.*, “Groundwater arsenic contamination in Ganga-Meghna-Brahmaputra plain, its health effects and an approach for mitigation,” *Environ. Earth Sci.*, vol. 70, no. 5, pp. 1993–2008, Nov. 2013, doi: 10.1007/s12665-013-2699-y.
- [32] D. Chakraborti, B. Das, and M. T. Murrill, “Examining India’s groundwater quality management,” *Environ. Sci. Technol.*, vol. 45, no. 1, pp. 27–33, Jan. 2011, doi: 10.1021/es101695d.
- [33] S. Srivastava and Y. K. Sharma, “Arsenic occurrence and accumulation in soil and water of eastern districts of Uttar Pradesh, India,” *Environ. Monit. Assess.*, vol. 185, no. 6, pp. 4995–5002, Jun. 2013, doi: 10.1007/s10661-012-2920-6.
- [34] D. Chakraborti *et al.*, “Fate of over 480 million inhabitants living in arsenic and fluoride endemic Indian districts: Magnitude, health, socio-economic effects and mitigation approaches,” *Journal of Trace Elements in Medicine and Biology*, vol. 38. Elsevier GmbH, pp. 33–45, Dec. 01,

2016, doi: 10.1016/j.jtemb.2016.05.001.

- [35] S. Ahamed *et al.*, “Arsenic groundwater contamination and its health effects in the state of Uttar Pradesh (UP) in upper and middle Ganga plain, India: A severe danger,” *Sci. Total Environ.*, vol. 370, no. 2–3, pp. 310–322, Nov. 2006, doi: 10.1016/j.scitotenv.2006.06.015.
- [36] W. R. Cullen and K. J. Reimer, “Arsenic Speciation in the Environment,” *Chem. Rev.*, vol. 89, no. 4, pp. 713–764, 1989, doi: 10.1021/cr00094a002.
- [37] J. F. Ferguson and J. Gavis, “A review of the arsenic cycle in natural waters,” *Water Res.*, vol. 6, no. 11, pp. 1259–1274, Nov. 1972, doi: 10.1016/0043-1354(72)90052-8.
- [38] and I. T. Y. Inam, Muhammad Ali, Rizwan Khan, Du Ri Park, Babar Aijaz Ali, Ahmed Uddin, “Influence of pH and Contaminant Redox Form on the Competitive Removal of Arsenic and Antimony from Aqueous Media by Coagulation,” *Minerals*, vol. 8, no. 12, p. 574, 2018.
- [39] I. Villaescusa and J. C. Bollinger, “Arsenic in drinking water: Sources, occurrence and health effects (a review),” *Reviews in Environmental Science and Biotechnology*, vol. 7, no. 4 SPEC. ISS. Springer, pp. 307–323, Dec. 09, 2008, doi: 10.1007/s11157-008-9138-7.
- [40] V. K. Sharma and M. Sohn, “Aquatic arsenic: Toxicity, speciation, transformations, and remediation,” *Environment International*, vol. 35, no. 4. Elsevier Ltd, pp. 743–759, 2009, doi: 10.1016/j.envint.2009.01.005.
- [41] J.-Q. Jiang, S. Ashekuzzaman, A. Jiang, S. Sharifuzzaman, and S. Chowdhury, “Arsenic Contaminated Groundwater and Its Treatment Options in Bangladesh,” *Int. J. Environ. Res. Public Health*, vol. 10, no. 1, pp. 18–46, Dec. 2012, doi: 10.3390/ijerph10010018.
- [42] Y. He, Y. P. Tang, D. Ma, and T. S. Chung, “UiO-66 incorporated thin-film nanocomposite membranes for efficient selenium and arsenic removal,” *J. Memb. Sci.*, vol. 541, pp. 262–270, Nov. 2017, doi: 10.1016/j.memsci.2017.06.061.

- [43] L. Hao, N. Wang, C. Wang, and G. Li, "Arsenic removal from water and river water by the combined adsorption - UF membrane process," *Chemosphere*, vol. 202, pp. 768–776, Jul. 2018, doi: 10.1016/j.chemosphere.2018.03.159.
- [44] H. Elcik, S. O. Celik, M. Cakmakci, and B. Özkaya, "Performance of nanofiltration and reverse osmosis membranes for arsenic removal from drinking water," *Desalin. Water Treat.*, vol. 57, no. 43, pp. 20422–20429, Sep. 2016, doi: 10.1080/19443994.2015.1111812.
- [45] S. A. Schmidt *et al.*, "Pilot study on arsenic removal from groundwater using a small-scale reverse osmosis system—Towards sustainable drinking water production," *J. Hazard. Mater.*, vol. 318, pp. 671–678, Nov. 2016, doi: 10.1016/j.jhazmat.2016.06.005.
- [46] C. Corroto, A. Iriel, A. F. Cirelli, and A. L. P. Carrera, "Constructed wetlands as an alternative for arsenic removal from reverse osmosis effluent," *Sci. Total Environ.*, vol. 691, pp. 1242–1250, Nov. 2019, doi: 10.1016/j.scitotenv.2019.07.234.
- [47] A. Sigdel, J. Park, H. Kwak, and P. K. Park, "Arsenic removal from aqueous solutions by adsorption onto hydrous iron oxide-impregnated alginate beads," *J. Ind. Eng. Chem.*, vol. 35, pp. 277–286, Mar. 2016, doi: 10.1016/j.jiec.2016.01.005.
- [48] M. A. Hashim *et al.*, "Arsenic removal by adsorption on activated carbon in a rotating packed bed," *J. Water Process Eng.*, vol. 30, p. 100591, Aug. 2019, doi: 10.1016/j.jwpe.2018.03.006.
- [49] L. K. Wu *et al.*, "Graphene oxide/CuFe₂O₄ foam as an efficient absorbent for arsenic removal from water," *Chem. Eng. J.*, vol. 334, pp. 1808–1819, Feb. 2018, doi: 10.1016/j.cej.2017.11.096.
- [50] A. Zouboulis and I. Katsoyiannis, "REMOVAL OF ARSENATES FROM CONTAMINATED WATER BY COAGULATION–DIRECT FILTRATION," *Sep. Sci. Technol.*, vol. 37, no. 12, pp. 2859–2873, Aug. 2002, doi: 10.1081/SS-120005470.
- [51] I. Kumar and A. R. Quaff, "Comparative study on the effectiveness of

- natural coagulant aids and commercial coagulant: removal of arsenic from water,” *Int. J. Environ. Sci. Technol.*, vol. 16, no. 10, pp. 5989–5994, Oct. 2019, doi: 10.1007/s13762-018-1980-8.
- [52] G. Jegadeesan, K. Mondal, and S. B. Lalvani, “Comparative study of selenite adsorption on carbon based adsorbents and activated alumina,” *Environ. Technol. (United Kingdom)*, vol. 24, no. 8, pp. 1049–1059, Aug. 2003, doi: 10.1080/09593330309385644.
- [53] Y. Zhang, M. Yang, and X. Huang, “Arsenic(V) removal with a Ce(IV)-doped iron oxide adsorbent,” *Chemosphere*, vol. 51, no. 9, pp. 945–952, Jun. 2003, doi: 10.1016/S0045-6535(02)00850-0.
- [54] S. Kuriakose, T. S. Singh, and K. K. Pant, “Adsorption of As(III) from aqueous solution onto iron oxide impregnated activated alumina,” *Water Qual. Res. J. Canada*, vol. 39, no. 3, pp. 258–266, Aug. 2004, doi: 10.2166/wqrj.2004.036.
- [55] L. S. McNeill and M. Edwards, “Soluble arsenic removal at water treatment plants,” *J. Am. Water Works Assoc.*, vol. 87, no. 4, pp. 105–113, Apr. 1995, doi: 10.1002/j.1551-8833.1995.tb06346.x.
- [56] J. G. Hering, P.-Y. Chen, J. A. Wilkie, and M. Elimelech, “Arsenic Removal from Drinking Water during Coagulation,” *J. Environ. Eng.*, vol. 123, no. 8, pp. 800–807, Aug. 1997, doi: 10.1061/(ASCE)0733-9372(1997)123:8(800).
- [57] A. Sarkar and B. Paul, “The global menace of arsenic and its conventional remediation - A critical review,” *Chemosphere*, vol. 158. Elsevier Ltd, pp. 37–49, Sep. 01, 2016, doi: 10.1016/j.chemosphere.2016.05.043.
- [58] G. Ungureanu, S. Santos, R. Boaventura, and C. Botelho, “Arsenic and antimony in water and wastewater: Overview of removal techniques with special reference to latest advances in adsorption,” *Journal of Environmental Management*, vol. 151. Academic Press, pp. 326–342, Mar. 05, 2015, doi: 10.1016/j.jenvman.2014.12.051.
- [59] S. Sorlini and F. Gialdini, “Conventional oxidation treatments for the

- removal of arsenic with chlorine dioxide, hypochlorite, potassium permanganate and monochloramine,” *Water Res.*, vol. 44, no. 19, pp. 5653–5659, Nov. 2010, doi: 10.1016/j.watres.2010.06.032.
- [60] R. Molinari and P. Argurio, “Arsenic removal from water by coupling photocatalysis and complexation-ultrafiltration processes: A preliminary study,” *Water Res.*, vol. 109, pp. 327–336, Feb. 2017, doi: 10.1016/j.watres.2016.11.054.
- [61] H. Lan *et al.*, “Efficient conversion of dimethylarsinate into arsenic and its simultaneous adsorption removal over FeCx/N-doped carbon fiber composite in an electro-Fenton process,” *Water Res.*, vol. 100, pp. 57–64, Sep. 2016, doi: 10.1016/j.watres.2016.05.018.
- [62] M. V. B. Krishna, K. Chandrasekaran, D. Karunasagar, and J. Arunachalam, “A combined treatment approach using Fenton’s reagent and zero valent iron for the removal of arsenic from drinking water,” *J. Hazard. Mater.*, vol. 84, no. 2–3, pp. 229–240, Jun. 2001, doi: 10.1016/S0304-3894(01)00205-9.
- [63] M. Lescano, C. Zalazar, A. Cassano, and R. Brandi, “Kinetic modeling of arsenic (III) oxidation in water employing the UV/H₂O₂ process,” *Chem. Eng. J.*, vol. 211–212, pp. 360–368, Nov. 2012, doi: 10.1016/j.cej.2012.09.075.
- [64] B. Rahimi and A. Ebrahimi, “Photocatalytic process for total arsenic removal using an innovative BiVO₄/TiO₂/LED system from aqueous solution: Optimization by response surface methodology (RSM),” *J. Taiwan Inst. Chem. Eng.*, vol. 101, pp. 64–79, Aug. 2019, doi: 10.1016/j.jtice.2019.04.036.
- [65] D. Mohan and C. U. Pittman, “Arsenic removal from water/wastewater using adsorbents-A critical review,” *Journal of Hazardous Materials*, vol. 142, no. 1–2. Elsevier, pp. 1–53, Apr. 02, 2007, doi: 10.1016/j.jhazmat.2007.01.006.
- [66] S. Ghosh (Nath), A. Debsarkar, and A. Dutta, “Technology alternatives for decontamination of arsenic-rich groundwater—A critical review,”

- Environmental Technology and Innovation*, vol. 13. Elsevier B.V., pp. 277–303, Feb. 01, 2019, doi: 10.1016/j.eti.2018.12.003.
- [67] R. Bain *et al.*, “Global assessment of exposure to faecal contamination through drinking water based on a systematic review,” *Trop. Med. Int. Heal.*, vol. 19, no. 8, pp. 917–927, Aug. 2014, doi: 10.1111/tmi.12334.
- [68] S. Abbaspour, “Water Quality in Developing Countries, South Asia, South Africa, Water Quality Management and Activities that Cause Water Pollution,” 2011.
- [69] “WHO | Assessing microbial safety of drinking water: Improving approaches and methods,” WHO, 2016, Accessed: Jun. 29, 2020. [Online]. Available: http://www.who.int/water_sanitation_health/publications/9241546301/en/.
- [70] W. Grabow, “Waterborne diseases: Update on water quality assessment and control.”
- [71] W. (World H. Organization)., *Guidelines for Drinking-water Quality THIRD EDITION INCORPORATING THE FIRST AND SECOND ADDENDA Volume 1 Recommendations Geneva 2008 WHO Library Cataloguing-in-Publication Data*. 2008.
- [72] H. Kulshrestha and S. Sharma, “Impact of mass bathing during Ardhkumbh on water quality status of river Ganga,” 2006. Accessed: Jun. 29, 2020. [Online]. Available: www.jeb.co.in.
- [73] V. Kumar, A. Sharma, A. K. Thukral, and R. Bhardwaj, “Water quality of River Beas, India,” 2017.
- [74] J. W. BHATTACHERJEE, S. P. PATHAK, and A. GAUR, “Antibiotic resistance and metal tolerance of coliform bacteria isolated from Gomati River water at Lucknow city.,” *J. Gen. Appl. Microbiol.*, vol. 34, no. 5, pp. 391–399, 1988, doi: 10.2323/jgam.34.391.
- [75] S. Skariyachan *et al.*, “Environmental monitoring of bacterial contamination and antibiotic resistance patterns of the fecal coliforms isolated from Cauvery River, a major drinking water source in

- Karnataka, India,” *Environ. Monit. Assess.*, vol. 187, no. 5, pp. 1–13, May 2015, doi: 10.1007/s10661-015-4488-4.
- [76] J. D. Van Elsas, A. V. Semenov, R. Costa, and J. T. Trevors, “Survival of *Escherichia coli* in the environment: Fundamental and public health aspects,” *ISME Journal*, vol. 5, no. 2. Nature Publishing Group, pp. 173–183, 2011, doi: 10.1038/ismej.2010.80.
- [77] S. Ishii, T. Yan, H. Vu, D. L. Hansen, R. E. Hicks, and M. J. Sadowsky, “Factors Controlling Long-Term Survival and Growth of Naturalized *Escherichia coli* Populations in Temperate Field Soils,” *Microbes Environ.*, vol. 25, no. 1, pp. 8–14, 2010, doi: 10.1264/jsme2.ME09172.
- [78] R. Jamieson, R. Gordon, K. Sharples, G. Stratton, and A. Madani, “Movement and persistence of fecal bacteria in agricultural soils and subsurface drainage water: A review,” 2002.
- [79] A. M. Ibekwe, A. Gonzalez-Rubio, and D. L. Suarez, “Impact of treated wastewater for irrigation on soil microbial communities,” *Sci. Total Environ.*, vol. 622–623, pp. 1603–1610, May 2018, doi: 10.1016/j.scitotenv.2017.10.039.
- [80] O. A. IJABADENIYI, L. K. DEBUSHO, M. VANDERLINDE, and E. M. BUYS, “IRRIGATION WATER AS A POTENTIAL PREHARVEST SOURCE OF BACTERIAL CONTAMINATION OF VEGETABLES,” *J. Food Saf.*, vol. 31, no. 4, pp. 452–461, Nov. 2011, doi: 10.1111/j.1745-4565.2011.00321.x.
- [81] L. Guo *et al.*, “Mechanism of virus inactivation by cold atmospheric-pressure plasma and plasmaactivated water,” *Appl. Environ. Microbiol.*, vol. 84, no. 17, Sep. 2018, doi: 10.1128/AEM.00726-18.
- [82] A. Lebedev, F. Anariba, J. C. Tan, X. Li, and P. Wu, “A review of physiochemical and photocatalytic properties of metal oxides against *Escherichia coli*,” *J. Photochem. Photobiol. A Chem.*, vol. 360, pp. 306–315, Jun. 2018, doi: 10.1016/j.jphotochem.2018.04.013.
- [83] K.-H. Kim and Y.-H. Kim, “A Review of Photocatalytic Treatment for Various Air Pollutants,” *Artic. Asian J. Atmos. Environ.*, 2011, doi:

10.5572/ajae.2011.5.3.181.

- [84] Y. Sun, Z. Zhang, and S. Wang, “Study on the Bactericidal Mechanism of Atmospheric-Pressure Low-Temperature Plasma against *Escherichia coli* and Its Application in Fresh-Cut Cucumbers,” *Molecules*, vol. 23, no. 4, 2018, doi: 10.3390/molecules23040975.
- [85] L. M. Da Silva and W. F. Jardim, “Trends and strategies of ozone application in environmental problems,” *Quim. Nova*, vol. 29, no. 2, pp. 310–317, Mar. 2006, doi: 10.1590/s0100-40422006000200023.
- [86] N. R. C. (US) S. D. W. Committee, “The Disinfection of Drinking Water,” 1980, Accessed: Jun. 30, 2020. [Online]. Available: <https://www.ncbi.nlm.nih.gov/books/NBK234590/>.
- [87] “Wastewater Technology Fact Sheet Ozone Disinfection,” 1999.
- [88] T. Zheng *et al.*, “A bibliometric analysis of micro/nano-bubble related research: current trends, present application, and future prospects,” *Scientometrics*, vol. 109, no. 1, pp. 53–71, Oct. 2016, doi: 10.1007/s11192-016-2004-4.
- [89] A. Agarwal, W. J. Ng, and Y. Liu, “Principle and applications of microbubble and nanobubble technology for water treatment,” *Chemosphere*, vol. 84, no. 9, Pergamon, pp. 1175–1180, Aug. 01, 2011, doi: 10.1016/j.chemosphere.2011.05.054.
- [90] T. Temesgen, T. T. Bui, M. Han, T. il Kim, and H. Park, “Micro and nanobubble technologies as a new horizon for water-treatment techniques: A review,” *Advances in Colloid and Interface Science*, vol. 246. Elsevier B.V., pp. 40–51, Aug. 01, 2017, doi: 10.1016/j.cis.2017.06.011.
- [91] S. W. Firman, K. Nirmala, E. Supriyono, and N. T. T. Rochman, “Performance evaluation of micro bubble generator on physiological response of Nile tilapia *Oreochromis niloticus* (Linnaeus, 1758) farmed at different densities in recirculating aquaculture system,” *J. Iktiologi Indones.*, vol. 19, no. 3, p. 425, Oct. 2019, doi: 10.32491/jii.v19i3.504.
- [92] M. FAN, D. TAO, R. HONAKER, and Z. LUO, “Nanobubble generation

- and its application in froth flotation (part I): nanobubble generation and its effects on properties of microbubble and millimeter scale bubble solutions,” *Min. Sci. Technol.*, vol. 20, no. 1, pp. 1–19, Jan. 2010, doi: 10.1016/S1674-5264(09)60154-X.
- [93] and J. L. Xing, Zhanwen, Jinrui Wang, Hengte Ke, Bo Zhao, Xiuli Yue, Zhifei Dai, “The fabrication of novel nanobubble ultrasound contrast agent for potential tumor imaging,” *Nanotechnology*, vol. 21, no. 14, 2010.
- [94] Y. Maeda, S. Hosokawa, Y. Baba, A. Tomiyama, and Y. Ito, “Generation mechanism of micro-bubbles in a pressurized dissolution method,” *Exp. Therm. Fluid Sci.*, vol. 60, pp. 201–207, Jan. 2015, doi: 10.1016/j.expthermflusci.2014.09.010.
- [95] H. Ohnari, “All about microbubbles,” *Nihin Jitsugyo Shuppanasha*, 2006.
- [96] M. Takahashi, K. Chiba, and P. Li, “Free-radical generation from collapsing microbubbles in the absence of a dynamic stimulus,” *J. Phys. Chem. B*, vol. 111, no. 6, pp. 1343–1347, Feb. 2007, doi: 10.1021/jp0669254.
- [97] L. Parkinson, R. Sedev, D. Fornasiero, and J. Ralston, “The terminal rise velocity of 10-100 μm diameter bubbles in water,” *J. Colloid Interface Sci.*, vol. 322, no. 1, pp. 168–172, Jun. 2008, doi: 10.1016/j.jcis.2008.02.072.
- [98] S. Ljunggren and J. C. Eriksson, “The lifetime of a colloid-sized gas bubble in water and the cause of the hydrophobic attraction,” *Colloids Surfaces A Physicochem. Eng. Asp.*, vol. 129–130, pp. 151–155, Nov. 1997, doi: 10.1016/S0927-7757(97)00033-2.
- [99] P. Arumugam, “Understanding the Fundamental Mechanisms of a Dynamic Micro-bubble Generator for Water Processing and Cleaning Applications,” 2015.
- [100] R. Parmar and S. K. Majumder, “Microbubble generation and microbubble-aided transport process intensification-A state-of-the-art

- report,” *Chemical Engineering and Processing: Process Intensification*, vol. 64, pp. 79–97, Feb. 2013, doi: 10.1016/j.cep.2012.12.002.
- [101] A. Fujiwara, K. Okamoto, K. Hashiguchi, J. Peixinho, S. Takagi, and Y. Matsumoto, “Bubble breakup phenomena in a venturi tube,” in *2007 Proceedings of the 5th Joint ASME/JSME Fluids Engineering Summer Conference, FEDSM 2007*, Mar. 2007, vol. 1 SYMPOSIA, no. PART A, pp. 553–560, doi: 10.1115/FEDSM2007-37243.
- [102] M. Takahashi, “Base and technological application of micro-bubble and nano-bubble,” *Mater. Integr.*, vol. 22, pp. 2–19, 2009.
- [103] H. Li, L. Hu, D. Song, and A. Al-Tabbaa, “Subsurface transport behavior of micro-nano bubbles and potential applications for groundwater remediation,” *Int. J. Environ. Res. Public Health*, vol. 11, no. 1, pp. 473–486, Dec. 2013, doi: 10.3390/ijerph110100473.
- [104] W. Xiao and G. Xu, “Mass transfer of nanobubble aeration and its effect on biofilm growth: Microbial activity and structural properties,” *Sci. Total Environ.*, vol. 703, p. 134976, Feb. 2020, doi: 10.1016/j.scitotenv.2019.134976.
- [105] Y. Sun, S. Wang, and J. Niu, “Microbial community evolution of black and stinking rivers during in situ remediation through micro-nano bubble and submerged resin floating bed technology,” *Bioresour. Technol.*, vol. 258, pp. 187–194, Jun. 2018, doi: 10.1016/j.biortech.2018.03.008.
- [106] S. Khuntia, S. K. Majumder, and P. Ghosh, “Adsorption of As(V) on zirconium-based adsorbents,” *Desalin. Water Treat.*, vol. 57, no. 4, pp. 1766–1778, Jan. 2016, doi: 10.1080/19443994.2014.978389.
- [107] M. D. Sharifuzzaman, H. N. Yang, S. M. Park, and K. J. Park, “Performance comparison of micro-nano bubble, electro-oxidation and ozone pre-treatment in reducing fluoride from industrial wastewater,” *Eng. Agric. Environ. Food*, vol. 10, no. 3, pp. 186–190, Jul. 2017, doi: 10.1016/j.eaef.2017.01.005.
- [108] S. Mauladani *et al.*, “Economic feasibility study of *Litopenaeus vannamei* shrimp farming: nanobubble investment in increasing harvest

- productivity,” *J. Akuakultur Indones.*, vol. 19, no. 1, pp. 30–38, Apr. 2020, doi: 10.19027/jai.19.1.30-38.
- [109] Y. Liu *et al.*, “Micro-nano bubble water oxygation: Synergistically improving irrigation water use efficiency, crop yield and quality,” *J. Clean. Prod.*, vol. 222, pp. 835–843, Jun. 2019, doi: 10.1016/j.jclepro.2019.02.208.
- [110] H. He, L. Zheng, Y. Li, and W. Song, “Research on the Feasibility of Spraying Micro/Nano Bubble Ozonated Water for Airborne Disease Prevention,” *Ozone Sci. Eng.*, vol. 37, no. 1, pp. 78–84, Jan. 2015, doi: 10.1080/01919512.2014.913473.
- [111] H. Sang, X. Jiao, S. Wang, W. Guo, M. K. Salahou, and K. Liu, “Effects of micro-nano bubble aerated irrigation and nitrogen fertilizer level on tillering, nitrogen uptake and utilization of early rice,” *Plant, Soil Environ.*, vol. 64 (2018), no. No. 7, pp. 297–302, Jun. 2018, doi: 10.17221/240/2018-PSE.
- [112] M. Sumikura, M. Hidaka, H. Murakami, Y. Nobutomo, and T. Murakami, “Ozone micro-bubble disinfection method for wastewater reuse system,” in *Water Science and Technology*, 2007, vol. 56, no. 5, pp. 53–61, doi: 10.2166/wst.2007.556.
- [113] D. Menendez and J. Valverde Flores, “Reduction of hospital wastewater through ozone-air micro-nanobubbles,” *J. Nanotechnol.*, vol. 1, no. 2, p. 59, Jan. 2018, doi: 10.32829/nanoj.v1i2.40.
- [114] R. D. R. Silva, R. T. Rodrigues, A. C. Azevedo, and J. Rubio, “Calcium and magnesium ion removal from water feeding a steam generator by chemical precipitation and flotation with micro and nanobubbles,” *Environ. Technol. (United Kingdom)*, 2019, doi: 10.1080/09593330.2018.1558288.
- [115] A. I. Rahmawati *et al.*, “Enhancement of *Penaeus vannamei* shrimp growth using nanobubble in indoor raceway pond,” *Aquac. Fish.*, Apr. 2020, doi: 10.1016/j.aaf.2020.03.005.
- [116] K. Jainontee *et al.*, “Preliminary Study of the Effects of Air-fine

- (Micro/Nano) Bubbles (FB) on the Growth Rate of Tilapia in Phan District, Chiang Rai, Thailand,” *Int. J. Plasma Environ. Sci. Technol.*, vol. 12, no. 2, 2019.
- [117] M. Takahashi, “ ζ Potential of microbubbles in aqueous solutions: Electrical properties of the gas - Water interface,” *J. Phys. Chem. B*, vol. 109, no. 46, pp. 21858–21864, Nov. 2005, doi: 10.1021/jp0445270.
- [118] G. H. Kelsall, S. Tang, S. Yurdakul, and A. L. Smith, “Electrophoretic behaviour of bubbles in aqueous electrolytes,” *J. Chem. Soc. - Faraday Trans.*, vol. 92, no. 20, pp. 3887–3893, Oct. 1996, doi: 10.1039/ft9969203887.
- [119] F. Y. Ushikubo *et al.*, “Evidence of the existence and the stability of nano-bubbles in water,” *Colloids Surfaces A Physicochem. Eng. Asp.*, vol. 361, no. 1–3, pp. 31–37, May 2010, doi: 10.1016/j.colsurfa.2010.03.005.
- [120] K. Terasaka, A. Hirabayashi, T. Nishino, S. Fujioka, and D. Kobayashi, “Development of microbubble aerator for waste water treatment using aerobic activated sludge,” *Chem. Eng. Sci.*, vol. 66, no. 14, pp. 3172–3179, Jul. 2011, doi: 10.1016/j.ces.2011.02.043.
- [121] J. S. Park and K. Kurata, “Application of microbubbles to hydroponics solution promotes lettuce growth,” *Horttechnology*, vol. 19, no. 1, pp. 212–215, Jan. 2009, doi: 10.21273/hortsci.19.1.212.
- [122] C. JIANG Shu-yi, CAO Guang-bin, HAN Shi-cheng, LIU Yong (Heilongjiang River Fisheries Research Institute, Chinese Academy of Fishery Sciences, Harbin 150070, “Optimal numerical studied on aerating oxygen bubbles in aquaculture,” *J. Dalian Fish. Univ.*, 2005.
- [123] K. B. Jenkins, D. L. Michelsen, and J. T. Novak, “Application of oxygen microbubbles for in situ biodegradation of p-xylene-contaminated groundwater in a soil column,” *Biotechnol. Prog.*, vol. 9, no. 4, pp. 394–400, Jul. 1993, doi: 10.1021/bp00022a006.
- [124] M. Parhizkar, M. Edirisinghe, and E. Stride, “The effect of surfactant type and concentration on the size and stability of microbubbles

- produced in a capillary embedded T-junction device,” *RSC Adv.*, vol. 5, no. 14, pp. 10751–10762, Jan. 2015, doi: 10.1039/c4ra15167d.
- [125] Q. Wang, H. Zhao, N. Qi, Y. Qin, X. Zhang, and Y. Li, “Generation and Stability of Size-Adjustable Bulk Nanobubbles Based on Periodic Pressure Change,” *Sci. Rep.*, vol. 9, no. 1, pp. 1–9, Dec. 2019, doi: 10.1038/s41598-018-38066-5.
- [126] M. OKUMURA, K. FUJINAGA, Y. SEIKE, and K. HAYASHI, “A Simple in situ Preconcentration Method for Phosphate Phosphorus in Environmental Waters by Column Solid Phase Extraction Using Activated Carbon Loaded with Zirconium.,” *Anal. Sci.*, vol. 14, no. 2, pp. 417–419, 1998, doi: 10.2116/analsci.14.417.
- [127] S. Y. Pang, J. Jiang, and J. Ma, “Oxidation of sulfoxides and arsenic(III) in corrosion of nanoscale zero valent iron by oxygen: Evidence against ferryl ions (Fe(IV)) as active intermediates in fenton reaction,” *Environ. Sci. Technol.*, vol. 45, no. 1, pp. 307–312, Jan. 2011, doi: 10.1021/es102401d.
- [128] J. Hoigné and H. Bader, “The role of hydroxyl radical reactions in ozonation processes in aqueous solutions,” *Water Res.*, vol. 10, no. 5, pp. 377–386, Jan. 1976, doi: 10.1016/0043-1354(76)90055-5.
- [129] L. Hu and Z. Xia, “Application of ozone micro-nano-bubbles to groundwater remediation,” *J. Hazard. Mater.*, vol. 342, pp. 446–453, Jan. 2018, doi: 10.1016/j.jhazmat.2017.08.030.
- [130] O. N, G. Zhang, and C. Yang, “Arsenic removal from waste water by ozone oxidation combined with ferric precipitation,” *Mong. J. Chem.*, vol. 17, no. 43, pp. 18–22, Feb. 2017, doi: 10.5564/mjc.v17i43.741.
- [131] J. H. Batagoda, S. D. A. Hewage, and J. N. Meegoda, “Remediation of heavy-metal-contaminated sediments in USA using ultrasound and ozone nanobubbles,” *J. Environ. Eng. Sci.*, vol. 14, no. 2, pp. 130–138, Jun. 2019, doi: 10.1680/jenes.18.00012.
- [132] C. A. B. and M. Lou Tortorello, *Encyclopedia of Food Microbiology / ScienceDirect*. .

- [133] T. V. Suslow, "Oxidation-Reduction Potential (ORP) for Water Disinfection Monitoring, Control, and Documentation PUBLICATION 8149 UNIVERSITY OF CALIFORNIA Division of Agriculture and Natural Resources." Accessed: Jun. 29, 2020. [Online]. Available: <http://anrcatalog.ucdavis.edu>.
- [134] M. Guo, H. Hu, J. R. Bolton, and M. G. El-Din, "Comparison of low- and medium-pressure ultraviolet lamps: Photoreactivation of *Escherichia coli* and total coliforms in secondary effluents of municipal wastewater treatment plants," *Water Res.*, vol. 43, no. 3, pp. 815–821, Feb. 2009, doi: 10.1016/j.watres.2008.11.028.
- [135] E. Alpaydin, *Introduction to Machine Learning, Third Edition*. 2020.
- [136] D. Steinberg, "CART: classification and regression trees," in *The Top Ten Algorithms in Data Mining*, Chapman and Hall/CRC, 2009.

Piniseti Swami Sairam

EDUCATION

- 2013-2015 M.Tech in Robotics Engineering, University of Petroleum & Energy Studies (UPES), Dehradun
- 2009-2013 B.Tech in Electronics and Communication Engineering, Vishnu Institute of Technology affiliated to JNTU-Kakinada, Bhimavaram, Andhra Pradesh

FUNDED PROJECTS

Project Title	Funding Agency	Amount
Sustainable system for removal of arsenic from water using Ozone Micro Nano Bubbles	Department of Science and Technology, Govt. of India	Rs. 30 Lakhs
Aquaculture growth study using Micro Nano Bubbles	SEED Research Grant, University of Petroleum and Energy Studies	Rs. 8 Lakhs

JOURNAL PUBLICATIONS

- P.S. Sairam, R. Gunupuru, A. Mehrotra, S.P. Singh, J.K. Pandey, Parameters influencing size of micro nano bubble, Int. J. Innov. Technol. Explor. Eng. 8 (2019) 3628–3630. doi:10.35940/ijitee.L3808.1081219.
- P.S. Sairam, R. Gunupuru, J.K. Pandey, Machine Learning Based Decision-Making Model to Determine Size of Micro Nano Bubble, Int. J. Recent Technol. Eng. 8 (2019) 8062–8064. doi:10.35940/ijrte.C6432.098319

CONFERENCE

“Nanobubbles: Exploring New Horizons for Betterment of Society”, poster presented at 6th International Conference on Hands-on Science, HSCI2019, held at National Technical University “Kharkiv Polytechnic Institute”, Ukraine.

Thesis

ORIGINALITY REPORT

% 9	% 6	% 8	% 3
SIMILARITY INDEX	INTERNET SOURCES	PUBLICATIONS	STUDENT PAPERS

PRIMARY SOURCES

1	Rajeev Parmar, Subrata Kumar Majumder. "Microbubble generation and microbubble-aided transport process intensification—A state-of-the-art report", Chemical Engineering and Processing: Process Intensification, 2013 Publication	%2
2	www.ijitee.org Internet Source	%1
3	cest.gnest.org Internet Source	%1
4	gutpathogens.biomedcentral.com Internet Source	%1
5	Mehmet Kobya, Reza Darvishi Cheshmeh Soltani, Philip Isaac Omwene, Alireza Khataee. "A review on decontamination of arsenic-contained water by electrocoagulation: Reactor configurations and operating cost along with removal mechanisms", Environmental Technology & Innovation, 2020 Publication	%1